UNIVERSIDAD DE CONCEPCIÓN

Centro de Investigación en Ingeniería Matemática (CI^{2}MA)

Implicit-explicit schemes for nonlinear nonlocal equations with a gradient flow structure in one space dimension

Raimund Bürger, Daniel Inzunza,
Pep Mulet, Luis M. Villada

PREPRINT 2018-20

SERIE DE PRE-PUBLICACIONES

IMPLICIT-EXPLICIT SCHEMES FOR NONLINEAR NONLOCAL EQUATIONS WITH A GRADIENT FLOW STRUCTURE IN ONE SPACE DIMENSION

RAIMUND BÜRGER[A,*], DANIEL INZUNZA[A], PEP MULET[B], AND LUIS MIGUEL VILLADA[C]

Abstract. Nonlinear convection-diffusion equations with nonlocal flux and possibly degenerate diffusion arise in various contexts including interacting gases, porous media flows, and collective behavior in biology. Their numerical solution by an explicit finite difference method is costly due to the necessity of discretizing a local spatial convolution for each evaluation of the convective numerical flux, and due to the disadvantageous Courant-Friedrichs-Lewy (CFL) condition incurred by the diffusion term. Based on explicit schemes for such models devised in [J.A. Carrillo, A. Chertock, Y. Huang, Commun. Comput. Phys. vol. 17 (2015) pp. 233–258] a second-order implicit-explicit Runge-Kutta (IMEX-RK) method can be formulated. This method avoids the restrictive time step limitation of explicit schemes since the diffusion term is handled implicitly, but entails the necessity to solve nonlinear algebraic systems in every time step. It is proved that this method is well defined. Numerical experiments illustrate that for fine discretizations it is more efficient in terms of reduction of error versus CPU time than the original explicit method. One of the test cases is given by a strongly degenerate parabolic, nonlocal equation modelling aggregation [F. Betancourt, R. Bürger, K.H. Karlsen, Commun. Math. Sci. vol. 9 (2011) pp. 711–742]. This model can be transformed to a local partial differential equation that can be solved numerically easily to generate a reference solution for the IMEX-RK method, but is limited to one space dimension.

1. Introduction

1.1. **Scope.** This paper is concerned with numerical methods for a nonlinear nonlocal equations with a gradient flow structure of the type

$$u_t + \nabla \cdot \big(u \nabla (W * u)\big) = \nabla \cdot \big(u \nabla (H'(u))\big), \quad \boldsymbol{x} \in \mathbb{R}^d, \quad t > 0, \tag{1.1}$$

$$u(\boldsymbol{x}, 0) = u_0(\boldsymbol{x}), \quad \boldsymbol{x} \in \mathbb{R}^d, \tag{1.2}$$

where $u(\boldsymbol{x}, t) \geq 0$ is an unknown probability distribution function or population density, $W(\boldsymbol{x})$ is an interaction potential, which is assumed to be symmetric, and $H(u)$ is a density of internal energy. This equation is a reduced variant of a more general equation (including an additional term) studied in [1]. Equations such as (1.1) appear in various contexts such as interacting gases, porous media flows and collective behavior in biology (see Section 1.2 and [1] for references). Clearly, if $W = 0$, and $H(u) = u \log u - u$ or $H(u) = u^m$, the classical heat equation and porous medium/fast diffusion equation are recovered, respectively [2]. The function W is related to the interaction energy (see below), and may be as singular as the Newtonian potential in the chemotaxis system [3] or as smooth as $W(\boldsymbol{x}) = |\boldsymbol{x}|^\alpha$ with $\alpha > 2$ in granular flow [4].

Date: April 17, 2018.

2010 *Mathematics Subject Classification.* 35K15, 35K55, 35K65, 65M06.

Key words and phrases. Nonlocal partial differential equation, gradient flow, implicit-explicit numerical method, aggregation model.

*Corresponding author.

[A]CI^{2}MA and Departamento de Ingeniería Matemática, Facultad de Ciencias Físicas y Matemáticas, Universidad de Concepción, Casilla 160-C, Concepción, Chile. E-Mail: rburger@ing-mat.udec.cl, dinzunza@ing-mat.udec.cl.

[B]Departament de Matemàtiques, Universitat de València, Av. Vicent Andrés Estellés, E-46100 Burjassot, Spain. E-Mail: mulet@uv.es.

[C]GIMNAP-Departamento de Matemáticas, Universidad del Bío-Bío, Casilla 5-C, Concepción, Chile, and CI^{2}MA, Universidad de Concepción, Casilla 160-C, Concepción, Chile. E-Mail: lvillada@ubiobio.cl.

In the present paper, we limit the discussion to the case of $d = 1$ space dimension, for which (1.1), (1.2) reduce to

$$u_t = F[u]_x, \quad x \in \mathbb{R}, \quad t > 0; \quad F[u] = u(H'(u) - W * u)_x, \tag{1.3}$$

$$u(x, 0) = u_0(x), \quad x \in \mathbb{R}. \tag{1.4}$$

Here the notation $F[u] = F[u(\cdot, t)]$ means that the flux F depends on $u(\cdot, t)$ as a function of x as a whole, and we recall that

$$\big(W * u(\cdot, t)\big)(x) = \int_{\mathbb{R}} W(y)u(x - y, t)\,\mathrm{d}y = \int_{\mathbb{R}} W(x - y)u(y, t)\,\mathrm{d}y.$$

Although the available mathematical theory does not allow us to be conclusive about the existence, uniqueness and well-posedness of the solution of such convection-diffusion equations, it is plausible to perform simulations with appropriate numerical methods. Explicit schemes for hyperbolic first-order conservation laws are widely used in many applications nowadays. Although they can be rather slow for some steady-state computations, due to CFL stability restrictions on the time step size, their use for unsteady computations is deemed as practical in many situations. When diffusion terms are present, one can resort to an implicit treatment of these terms to overcome the drastic step size stability restrictions imposed by their alternative explicit treatment. It is the purpose of the present work to demonstrate the benefits of using an implicit-explicit (IMEX) scheme for the efficient solution of (1.3), (1.4) under specific assumptions on the diffusive term. It is shown that the proposed scheme is more efficient, in terms of error reduction versus CPU time, than the explicit scheme of [1].

1.2. **Related work.** Equation (1.1), or some specific case of it, arises in many contexts including interacting gases [5], granular flows [6], flow in porous media [7,8], and collective behavior in biology [9] (see these papers and [1] for further references). The one-dimensional model (1.3), (1.4) can also be understood as a model of the aggregation of populations by the following reasoning [10]. Assume that u is the density of the population (e.g., of animals) under study, and consider the equation

$$u_t + \left(-k\left[\int_{-\infty}^{x} u(y, t)\,\mathrm{d}y - \int_{x}^{\infty} u(y, t)\,\mathrm{d}y\right]u\right)_x = A(u)_{xx}, \quad x \in \mathbb{R}, \quad t > 0. \tag{1.5}$$

Here $k > 0$ is a constant, and the convective term models that an animal will move to the right (respectively, left) if the total population to its right is larger (respectively, smaller) than to its left. The aggregation mechanism is balanced by nonlinear diffusion described by the term $A(u)_{xx}$, known as density-dependent dispersal in mathematical ecology [10], where $A(u) = \int_0^u a(s)\,\mathrm{d}s$ and $a(u) \geq 0$ is a given diffusion function Properties of (1.5) under various assumptions on the regularity of a were studied in [10–16]. As in [10, 11] we allow that $a(u)$ may vanish on u-intervals of positive length, so (1.5) may be strongly degenerate. To see that (1.5) is an example of (1.3), we first rewrite (1.5) as

$$u_t + (u\tilde{W} * u)_x = A(u)_{xx} \tag{1.6}$$

with the odd kernel $\tilde{W}(x) = -k\,\mathrm{sgn}(x)$. Equation (1.6) becomes a one-dimensional example of (1.1) if we observe that $\tilde{W} * u = W' * u$, where W' denotes the derivative of W, if we choose the even kernel $W(x) = k|x| + C$, where C is a constant and the function H is given by

$$H(u) = \int_0^u \int_0^r \frac{a(s)}{s}\,\mathrm{d}s\,\mathrm{d}r$$

(where possibly further restrictions on the function $u \mapsto a(u)$ need to be imposed so that H is well defined). The particular interest in this degenerate nonlocal aggregation equation arises from the numerical method for its solution constructed in [10], where the general equation

$$u_t + \left(\Phi'\left(\int_{-\infty}^{x} u(y, t)\,\mathrm{d}y\right)u\right)_x = A(u)_{xx} \tag{1.7}$$

is analyzed. If the function Φ is chosen such that $\Phi'(q) = -k(2q - C_0)$, where $C_0 = \int_{\mathbb{R}} u_0(x)\mathrm{d}x$, the equation (1.5) is obtained. The key observation here is that the primitive $q(x,t) := \int_{-\infty}^{x} u(y,t)\mathrm{d}y$ is a solution of the following initial value problem for a *local* PDE:

$$q_t + \Phi(q)_x = A(q_x)_x, \quad x \in \mathbb{R}, \quad t > 0; \quad q(x,0) = q_0(x) := \int_{-\infty}^{x} u_0(\xi)\,\mathrm{d}\xi, \quad x \in \mathbb{R}. \tag{1.8}$$

Thus, by solving the local problem (1.8) numerically, and transforming back the numerical solution to u, we may conveniently generate a reference solution (for this particular aggregation model) that does not involve a discretization of the convolution but that can be used to assess the performance of the numerical scheme developed herein that solves (1.3) directly, and in particular does involve calculating the convolution in every time step. See Section 3.4 for further details.

Concerning numerical methods for (1.1), we mention that finite element approximations have been proposed in the literature which are positivity preserving and entropy decreasing at the expense of constructing them by an implicit discretization in time but continuous in space [17]. We also mention that Carrillo, Chertock, and Huang [1] consider (1.3) adding the term $V(x)$ which represents a confinement potential, i.e.,

$$\rho_t(x) = \left(\rho\left(H'(\rho) + V(x) - W * \rho\right)_x\right)_x. \tag{1.9}$$

This a variant of (1.3) and has been extensively studied during the last fifteen years. In both cases of (1.3) and (1.9), the numerical methods studied for these equations are explicit schemes for convection-diffusion equations. In fact, Carrillo et al. [1] propose both one- and two-dimensional finite volume schemes for (1.1) and prove their positivity preserving and entropy dissipation properties along with error estimates and convergence results. These schemes follow a method of lines and are explicit by the choice of explicit SSP Runge-Kutta ODE integrators.

Although in [1] the detailed stability restriction for the proposed method, which implies that $\Delta t \propto \Delta x^2$, is not made apparent, in the experiments section we will show that it is indeed required. This restriction stems from the explicit treatment of the diffusive term, so this motivates the main goal of our work, which is to propose an implicit-explicit Runge-Kutta method (IMEX-RK method) that treats the diffusive term implicitly and the convective term explicitly. To explain the main idea, we consider the problem

$$\frac{\mathrm{d}\boldsymbol{u}}{\mathrm{d}t} = \boldsymbol{\mathcal{C}}(\boldsymbol{u}) + \boldsymbol{\mathcal{D}}(\boldsymbol{u}), \tag{1.10}$$

which is assumed to represent a method-of-lines semi-discretization of (1.1), where $\boldsymbol{u} = \boldsymbol{u}(t)$ is a spatial discretization of the solution and $\boldsymbol{\mathcal{C}}(\boldsymbol{u})$ and $\boldsymbol{\mathcal{D}}(\boldsymbol{u})$ are discretizations of the convective and diffusive terms, respectively. Assume, for simplicity, that the spatial mesh width is $\Delta x > 0$. Then the stability restriction on the time step Δt that explicit schemes impose when applied to (1.10) is very severe (Δt must be proportional to the square Δx^2 of the grid spacing), due the presence of $\boldsymbol{\mathcal{D}}(\boldsymbol{u})$. Implicit treatment of both $\boldsymbol{\mathcal{C}}(\boldsymbol{u})$ and $\boldsymbol{\mathcal{D}}(\boldsymbol{u})$ would remove any stability restriction on Δt. However, the upwind nonlinear discretization of the convective terms contained in $\boldsymbol{\mathcal{C}}(\boldsymbol{u})$ that is needed for stability, makes its implicit treatment extremely involved. In fact, after the pioneering work of Crouzeix [18], numerical integrators that deal implicitly with $\boldsymbol{\mathcal{D}}(\boldsymbol{u})$ and explicitly with $\boldsymbol{\mathcal{C}}(\boldsymbol{u})$ can be used with a time step restriction dictated by the convective term alone. These schemes, apart from having been profusely used in convection-diffusion problems and convection problems with stiff reaction term [19, 20], have been used recently to deal with stiff terms in hyperbolic systems with relaxation [21–25]. Finally, we mention that many authors have proposed IMEX-RK scheme for the solution of semidiscretized PDEs [19, 21, 26–30].

1.3. **Outline of the paper.** The remainder of this work is organized as follows. In Section 2 we introduce the numerical scheme. We use the method of lines to obtain a spatial semi-discretization of (1.3) in form of a system of ordinary differential equations (ODEs) that involves a clear definition of convective and diffusive numerical fluxes (Section 2.1). In particular the convective term is discretized via MUSCL extrapolation applied to an upwind scheme, as introduced in [1]. Then, in Section 2.2, we demonstrate that an explicit first-order (Euler) time discretization leads to a positivity preserving scheme (Theorem 2.1). In Section 2.3 we briefly motivate the advantage of using IMEX-RK time integrators for the problem at hand, and in Section 2.4 we specify the particular IMEX-RK time integrators used to solve the system of ODEs that

represents the spatial discretization. The implementation of this scheme requires the solution of nonlinear algebraic equations in each time step. The existence of a unique solution of these equations is a consequence of a fixed-point theorem that is proved in Section 2.4 (Theorem 2.2). For the special case of the simplest IMEX scheme, namely the Euler IMEX scheme, this result entails that the whole scheme is positivity preserving, as is shown in Theorem 2.3. In Section 3 the presented numerical results (Examples 1 to 4) indicate that in most circumstances the IMEX-RK scheme is significantly more efficient in reduction of error versus CPU time than the explicit scheme developed in [1]. These and other conclusions are summarized in Section 4.

2. Numerical method

2.1. **Spatial discretization.** For the one-dimensional equation (1.3) we consider a spatial domain $\Omega = (-L, L)$ large enough so that the solution is compactly supported in it. We also consider a subdivision of Ω into M cells $C_j = [x_{j-1/2}, x_{j+1/2}]$ of a uniform size Δx with $x_j = -L + (j - 1/2)\Delta x$, $j \in \{1, \dots, M\}$, $x_{j\pm1/2} = x_j \pm \Delta x/2$, and denote by $u_j(t)$ an approximation to the solution cell average on C_j, i.e.,

$$u_j(t) \approx \frac{1}{\Delta x} \int_{x_{j-1/2}}^{x_{j+1/2}} u(x,t)\,\mathrm{d}x.$$

To obtain a semi-discrete finite volume scheme, (1.3) is first integrated over the j-th cell to give

$$\frac{\mathrm{d}}{\mathrm{d}t}\left(\int_{x_{j-1/2}}^{x_{j+1/2}} u(x,t)\,\mathrm{d}x\right) = F[u(\cdot,t)](x_{j+1/2}) - F[u(\cdot,t)](x_{j-1/2}).$$

We divide this equation by Δx and approximate the terms $\hat{F}_{j\pm1/2}(t) \approx F[u(\cdot,t)](x_{j\pm1/2})$ by some numerical flux function $\hat{F}$ with arguments chosen among the variables u_l within some finite stencil around j,

$$\hat{F}_{j+1/2}(t) = \hat{F}\big(u_{j-p}(t), \dots, u_{j+q}(t)\big).$$

Then the final semidiscrete scheme takes the form of the following system of ODEs for u_j (notice that the signs are reversed with respect to the standard notation in conservation laws):

$$u_j'(t) = \frac{\hat{F}_{j+1/2}(t) - \hat{F}_{j-1/2}(t)}{\Delta x}. \tag{2.1}$$

For our separate treatment of convective and diffusive terms, we split $F[u]$ as follows:

$$F[u] = uH''(u)u_x - u(W * u)_x = K(u)_x - u(W * u)_x, \quad K'(u) = uH''(u), \tag{2.2}$$

where we assume the following properties of K:

$$\begin{aligned} &K \text{ is at least twice continuously differentiable,}\\ &K(0) = 0,\\ &K'(u) \geq 0, K''(u) \geq 0 \text{ for } u \in (0,\infty),\\ &K(u) = uL(u), \text{ with } L \text{ continuous in } [0,\infty). \end{aligned} \tag{2.3}$$

In particular, $K(u) \geq 0$ for $u \geq 0$.

Now we approximate both terms in (2.2) separately, omitting the dependence of quantities on $t \geq 0$ for sake of simplicity. The diffusive term is approximated by standard second-order three-point finite differences:

$$K(u)_x(x_j) \approx \frac{K(u_{j+1}) - 2K(u_j) + K(u_{j-1})}{\Delta x^2} = \frac{1}{\Delta x}\big(\hat{F}^{\mathrm{d}}_{j+1/2} - \hat{F}^{\mathrm{d}}_{j-1/2}\big), \quad \hat{F}^{\mathrm{d}}_{j+1/2:} = \frac{K(u_{j+1}) - K(u_j)}{\Delta x}.$$

Regarding the convective term, the flux can be expressed as

$$uv[u], \quad v[u] = z[u]_x, \quad z[u] = W * u. \tag{2.4}$$

We use MUSCL reconstructions [31] and standard upwind techniques to obtain the convective numerical flux. One first constructs piecewise linear polynomials in each cell C_j, namely

$$\tilde{u}_j(x) = u_j + \sigma_j(x - x_j), \quad x \in C_j, \tag{2.5}$$

and computes right and left point values, u_j^{R} and u_j^{L}, at the cell respective interfaces $x_{j+1/2}$ and $x_{j-1/2}$, by

$$u_j^{\mathrm{R}} = \tilde{u}_j\big(x_{j+1/2}^-\big) = u_j + \frac{\Delta x}{2}\sigma_j, \quad u_j^{\mathrm{L}} = \tilde{u}_j\big(x_{j-1/2}^+\big) = u_j - \frac{\Delta x}{2}\sigma_j. \tag{2.6}$$

These values will be second-order accurate provided the slopes σ_j are at least first-order accurate approximations of the partial derivative $u_x(x,\cdot)$. To ensure that the point values (2.6) are both second-order accurate and nonnegative, the slopes σ_j in (2.5) are calculated as follows. First, the centered difference approximation $\sigma_j = (u_{j+1} - u_{j-1})/(2\Delta x)$ is used for all j. Then, if a reconstructed point value at a cell boundary becomes negative (i.e., either $u_j^{\mathrm{R}} < 0$ or $u_j^{\mathrm{L}} < 0$), we correct the corresponding slope σ_j using a slope limiter, which guarantees that the reconstructed point values are nonnegative as long as the cell averages u_j are nonnegative. In the numerical experiments in [1] this is achieved by using a minmod limiter as follows:

$$\sigma_j = \begin{cases} \dfrac{u_{j+1} - u_{j-1}}{2\Delta x} & \text{if } u_j \geq \dfrac{|u_{j+1} - u_{j-1}|}{4\Delta x}, \\ \theta\,\mathrm{minmod}\left(\dfrac{u_{j+1} - u_j}{\Delta x}, \dfrac{u_j - u_{j-1}}{\Delta x}\right) & \text{otherwise,} \end{cases}$$

where the standard minmod function is defined as

$$\mathrm{minmod}(z_1, z_2) := \begin{cases} \mathrm{sgn}(z_1)\min\{|z_1|, |z_2|\} & \text{if } \mathrm{sgn}(z_1) = \mathrm{sgn}(z_2), \\ 0 & \text{otherwise,} \end{cases}$$

and the parameter $\theta \in (0, 2]$ is used to control the numerical viscosity of the resulting scheme. The value $\theta = 2$ is used for the numerical examples in [1], and we adopt it in all our numerical examples.

To approximate $v[u](x_{j+1/2})$, we first use a second-order finite difference formula

$$z[u]_x(x_{j+1/2}) \approx \frac{z[u](x_{j+1}) - z[u](x_j)}{\Delta x}, \tag{2.7}$$

followed by discrete approximations of the convolutions $(W * u)(x_j)$, taking into account that u is compactly supported in $(-L, L)$, given by

$$(W * u)(x_j) = z[u](x_j) \approx \tilde{z}[u]_j = \tilde{z}[u_{j-s}^*, \ldots, u_{j+s}^*] = \Delta x \sum_{l=-s}^{s} W_l u_{j-l}^*, \tag{2.8}$$

where we define

$$u_l^* := \begin{cases} u_l & \text{if } 1 \leq l \leq M, \\ 0 & \text{otherwise,} \end{cases}$$

where $W_l = W(l\Delta x)$, and the width of the convolution stencil $s = s_{\Delta x}$ is computed to retain second-order accuracy. Clearly, the computational bottleneck in this procedure is the discrete convolution in (2.8). This is a classical problem in scientific computing that is effectively evaluated using fast convolution algorithms, mainly based on Fast Fourier Transforms [32]. These techniques are applied here within the IMEX-RK version as well as within the explicit methods of [1].

To recap, the following approximation, obtained from (2.7) and (2.8),

$$v[u](x_{j+1/2}) = z[u]_x(x_{j+1/2}) \approx v_{j+1/2} = \tilde{v}[u]_{j+1/2} = \frac{\tilde{z}[u]_{j+1} - \tilde{z}[u]_j}{\Delta x}, \tag{2.9}$$

yields, in an upwind manner, the convective numerical flux associated with the cell interface $x_{j+1/2}$, namely

$$\hat{F}_{j+1/2}^{\mathrm{c}} = u_{j+1/2} v_{j+1/2}, \quad \text{where} \quad u_{j+1/2} = \begin{cases} u_j^{\mathrm{R}} & \text{if } v_{j+1/2} \geq 0, \\ u_{j+1}^{\mathrm{L}} & \text{if } v_{j+1/2} < 0, \end{cases} \tag{2.10}$$

which we can write in closed form as

$$\hat{F}_{j+1/2}^{\mathrm{c}} = u_j^{\mathrm{R}} v_{j+1/2}^- + u_{j+1}^{\mathrm{L}} v_{j+1/2}^+, \tag{2.11}$$

where $v^+_{j+1/2} := \max\{v_{j+1/2}, 0\}$ and $v^-_{j+1/2} := \min\{v_{j+1/2}, 0\}$. We set

$$\hat{F}_{j+1/2} = -\hat{F}^{\mathrm{c}}_{j+1/2} + \hat{F}^{\mathrm{d}}_{j+1/2}$$

compatibly with the splitting (2.2), so that (1.10) with $\boldsymbol{u} = (u_1, \ldots, u_M)^{\mathrm{T}}$, $\boldsymbol{\mathcal{C}}(\boldsymbol{u}) = (\mathcal{C}_1(\boldsymbol{u}), \ldots, \mathcal{C}_M(\boldsymbol{u}))^{\mathrm{T}}$ and $\boldsymbol{\mathcal{D}}(\boldsymbol{u}) = (\mathcal{D}_1(\boldsymbol{u}), \ldots, \mathcal{D}_M(\boldsymbol{u}))^{\mathrm{T}}$ and (2.1) can be written as

$$u_j'(t) = \mathcal{C}_j(\boldsymbol{u}) + \mathcal{D}_j(\boldsymbol{u}), \quad \mathcal{C}_j(\boldsymbol{u}) := -\frac{\hat{F}^{\mathrm{c}}_{j+1/2} - \hat{F}^{\mathrm{c}}_{j-1/2}}{\Delta x}, \quad \mathcal{D}_j(\boldsymbol{u}) := \frac{\hat{F}^{\mathrm{d}}_{j+1/2} - \hat{F}^{\mathrm{d}}_{j-1/2}}{\Delta x}, \quad j = 1, \ldots, M. \tag{2.12}$$

It is worth pointing out that the original reference scheme in [1] is obtained through this procedure by taking $z[u] = H'(u) + W * u$ in (2.4) and $\hat{F}_{j+1/2} = \hat{F}^{\mathrm{c}}_{j+1/2}$.

2.2. **A property of an explicit time discretization.** The ODEs that form the semi-discrete scheme (2.1) need to be integrated numerically using a stable and accurate ODE solver. In all their numerical examples, Carrillo et al. [1] use the third-order strong stability preserving Runge-Kutta (SSP-RK) ODE solver [33]. The resulting scheme preserves positivity of the computed cell averages u_j, as stated in [1, Theorem 2.1]. Its proof is based on the forward Euler integration of (2.1), but it remains valid if the forward Euler method is replaced by a higher-order SSP-ODE solver [33], whose time step can be expressed as a convex combination of several forward Euler steps. For our scheme we can prove the following result, which is an analogue of [1, Theorem 2.1], following the lines stated therein.

Theorem 2.1. *If K is increasing and convex in $[0, \infty)$, $u_{j+1/2}$ in* (2.10) *is nonnegative, and the CFL condition*

$$\Delta t \left(\frac{\max_j |v_{j+1/2}|}{\Delta x} + \frac{\max_j K'(u_j)}{\Delta x^2} \right) \leq \frac{1}{2} \tag{2.13}$$

is satisfied, then the explicit Euler method applied to the semi-discrete scheme (2.12) *yields a fully discrete positivity preserving scheme, i.e.,*

$$\mathcal{E}(u)_j := u_j + \frac{\Delta t}{\Delta x}\big(\hat{F}_{j+1/2} - \hat{F}_{j-1/2}\big) \geq 0. \tag{2.14}$$

Proof. Since for $j = 1, \ldots, M$ $(u^{\mathrm{L}}_j + u^{\mathrm{R}}_j)/2 = u_j$ and there exists $\hat{u}_{j+1/2}$ such that

$$K(u_{j+1}) - K(u_j) = K'(\hat{u}_{j+1/2})(u_{j+1} - u_j),$$

by (2.11) and (2.12) the inequality (2.14) can be written as

$$\begin{aligned}
\mathcal{E}(u)_j &= \frac{u^{\mathrm{L}}_j + u^{\mathrm{R}}_j}{2} + \frac{\Delta t}{\Delta x}\big(-u^{\mathrm{R}}_j v^+_{j+1/2} - u^{\mathrm{L}}_{j+1} v^-_{j+1/2} + u^{\mathrm{R}}_{j-1} v^+_{j-1/2} + u^{\mathrm{L}}_j v^-_{j-1/2}\big) \\
&\quad + \frac{\Delta t}{\Delta x^2}\big(K(u_{j+1}) - 2K(u_j) + K(u_{j-1})\big) \\
&= \left(\frac{1}{2} + \frac{\Delta t}{\Delta x} v^-_{j-1/2}\right) u^{\mathrm{L}}_j + \left(\frac{1}{2} - \frac{\Delta t}{\Delta x} v^+_{j+1/2}\right) u^{\mathrm{R}}_j + \frac{\Delta t}{\Delta x}\big(-u^{\mathrm{L}}_{j+1} v^-_{j+1/2} + u^{\mathrm{R}}_{j-1} v^+_{j-1/2}\big) \\
&\quad + \frac{\Delta t}{\Delta x^2}\big(K'(\hat{u}_{j+1/2})(u_{j+1} - u_j) - K'(\hat{u}_{j-1/2})(u_j - u_{j-1})\big) \\
&= \left(\frac{1}{2} + \frac{\Delta t}{\Delta x} v^-_{j-1/2} - \frac{\Delta t}{2\Delta x^2}(K'(\hat{u}_{j+1/2}) + K'(\hat{u}_{j-1/2}))\right) u^{\mathrm{L}}_j \\
&\quad + \left(\frac{1}{2} - \frac{\Delta t}{\Delta x} v^+_{j+1/2} - \frac{\Delta t}{2\Delta x^2}\big(K'(\hat{u}_{j+1/2}) + K'(\hat{u}_{j-1/2})\big)\right) u^{\mathrm{R}}_j + \frac{\Delta t}{\Delta x}\big(u^{\mathrm{L}}_{j+1} v^+_{j+1/2} - u^{\mathrm{R}}_{j-1} v^-_{j-1/2}\big) \\
&\quad + \frac{\Delta t}{\Delta x^2}\Big(K'(\hat{u}_{j+1/2}) u_{j+1} + K'(\hat{u}_{j-1/2}) u_{j-1}\Big) \\
&\geq \left(\frac{1}{2} - \frac{\Delta t}{\Delta x} \max_j |v_{j-1/2}| - \frac{\Delta t}{\Delta x^2} \max_j K'(u_j)\right) u^{\mathrm{L}}_j + \left(\frac{1}{2} - \frac{\Delta t}{\Delta x} \max_j |v_{j-1/2}| - \frac{\Delta t}{\Delta x^2} \max_j K'(u_j)\right) u^{\mathrm{R}}_j \\
&\geq 0,
\end{aligned}$$

where we have taken into account that $K', K'' \geq 0$ to bound $K'(\hat{u}_{j+1/2}) \leq K'(\max(u_j, u_{j+1}))$. □

The following result provides usable bounds for the velocities in (2.13).

Lemma 2.1. *We have the following bounds:*

$$|v_{j+1/2}| \leq \|W\|_\infty \,\mathrm{TV}(u), \quad |v_{j+1/2}| \leq \|u\|_\infty \,\mathrm{TV}(W),$$

provided that the right-hand sides are finite.

Proof. These results follow directly from the definition of $v_{j+1/2}$ in (2.8) and (2.9). For instance,

$$v_{j+1/2} = \sum_{l=-s}^{s} W_l\big(u^*_{j+1-l} - u^*_{j-l}\big),$$

immediately yields the first bound. □

2.3. **Stability.** A rigorous study of von Neumann stability of explicit ODE solvers applied to (2.12) or the original scheme in [1] is not possible since the linearization of (1.3) does not have a structure amenable to this analysis. Nevertheless, the closest scenario permitting an stability analysis would be the application of a linear scheme to the standard convection diffusion equation

$$u_t + \gamma u_x = \eta u_{xx}, \tag{2.15}$$

where $\gamma \approx (W * u)_x$ and $\eta \approx K'(u)$. For some simple Runge-Kutta explicit schemes, it can be readily seen that such schemes applied to (2.15) are stable provided

$$\Delta t \left(\frac{\gamma}{\Delta x} + \frac{\eta}{\Delta x^2}\right) \leq C_1$$

for some constant C_1. This result is coherent with (2.13) and will be illustrated in the numerics section. This bound can be severely restrictive for fine simulations and is therefore a clear motivation for the consideration of implicit-explicit Runge-Kutta schemes, that typically relax the latter bound to $\gamma\Delta t/\Delta x \leq C_2$, a restriction that is fine for accuracy requirements.

2.4. **Implicit-explicit Runge-Kutta schemes.** For the diffusive part $\boldsymbol{\mathcal{D}}(\boldsymbol{u})$ we utilize an implicit s-stage diagonally implicit (DIRK) scheme with coefficients $\boldsymbol{A} \in \mathbb{R}^{s\times s}$, $\boldsymbol{b}, \boldsymbol{c} \in \mathbb{R}^s$, in the common Butcher notation, where $\boldsymbol{A} = (a_{ij})$ with $a_{ij} = 0$ for $j > i$. For the convective term $\boldsymbol{\mathcal{C}}(\boldsymbol{u})$ we employ an s-stage explicit scheme with coefficients $\tilde{\boldsymbol{A}} \in \mathbb{R}^{s\times s}$, $\tilde{\boldsymbol{b}}, \tilde{\boldsymbol{c}} \in \mathbb{R}^s$ and $\tilde{\boldsymbol{A}} = (\tilde{a}_{ij})$ with $\tilde{a}_{ij} = 0$ for $j \geq i$. We denote the corresponding Butcher arrays by

$$\boldsymbol{D} := \begin{array}{c|c} \boldsymbol{c} & \boldsymbol{A} \\ \hline & \boldsymbol{b}^{\mathrm{T}} \end{array}, \quad \tilde{\boldsymbol{D}} := \begin{array}{c|c} \tilde{\boldsymbol{c}} & \tilde{\boldsymbol{A}} \\ \hline & \tilde{\boldsymbol{b}}^{\mathrm{T}} \end{array}.$$

If applied to (2.12), the IMEX-RK scheme gives rise to the following algorithm, where we recall that $\boldsymbol{u} = (u_1, \ldots, u_M)^{\mathrm{T}}$, etc.:

Algorithm 3.1: IMEX-RK scheme

Input: approximate solution vector $\boldsymbol{u}^n$ for $t = t_n$
do $i = 1, \ldots, s$
solve for $\boldsymbol{u}^{(i)}$ the nonlinear equation

$$\boldsymbol{u}^{(i)} = \boldsymbol{u}^n + \Delta t\left(\sum_{j=1}^{i-1} a_{ij}\boldsymbol{\kappa}_j + \sum_{j=1}^{i-1} \tilde{a}_{ij}\tilde{\boldsymbol{\kappa}}_j\right) + a_{ii}\Delta t\boldsymbol{\mathcal{D}}\big(\boldsymbol{u}^{(i)}\big)$$

$\boldsymbol{\kappa}_i \leftarrow \boldsymbol{\mathcal{D}}\big(\boldsymbol{u}^{(i)}\big)$, $\tilde{\boldsymbol{\kappa}}_i \leftarrow \boldsymbol{\mathcal{C}}\big(\boldsymbol{u}^{(i)}\big)$
enddo

$$\boldsymbol{u}^{n+1} \leftarrow \boldsymbol{u}^n + \Delta t\sum_{j=1}^{s} b_j\,\boldsymbol{\kappa}_j + \Delta t\sum_{i=1}^{s} \tilde{b}_i\tilde{\boldsymbol{\kappa}}_i$$

Output: approximate solution vector $\boldsymbol{u}^{n+1}$ for $t = t^{n+1} = t^n + \Delta t$.

This algorithm requires solving for each $i \in \{1, \dots, s\}$ the nonlinear system

$$\boldsymbol{F}(\boldsymbol{u}) := \boldsymbol{u} - a_{ii}\Delta t D(\boldsymbol{u}) - \boldsymbol{r} = \boldsymbol{0}, \quad i = 1, \dots, s, \tag{2.16}$$

for the unknown vector $\boldsymbol{u} = \boldsymbol{u}^{(i)}$, where the vector $\boldsymbol{r}$ is given by

$$\boldsymbol{r} = \boldsymbol{u}^n + \Delta t \left(\sum_{j=1}^{i-1} a_{ij} \boldsymbol{\kappa}_j + \sum_{j=1}^{i-1} \tilde{a}_{ij} \tilde{\boldsymbol{\kappa}}_j \right). \tag{2.17}$$

The following results deal with the solution of (2.16).

Theorem 2.2. *Assume that K satisfies the conditions (2.3), $\mu > 0$, $\boldsymbol{c} \in \mathbb{R}^M$, and $\boldsymbol{c} \geq \boldsymbol{0}$, where such inequalities for vectors and matrices are understood in the component-wise sense. Then the equation*

$$\boldsymbol{z} - \mu \boldsymbol{\mathcal{D}}(\boldsymbol{z}) = \boldsymbol{c} \tag{2.18}$$

has a unique solution $\boldsymbol{z} \in \mathbb{R}^M$ satisfying $\boldsymbol{z} \geq \boldsymbol{0}$.

Proof. Equation (2.18) can be rewritten as

$$\boldsymbol{z} + \boldsymbol{G}\boldsymbol{K}(\boldsymbol{z}) = \boldsymbol{c}, \tag{2.19}$$

where the $M \times M$-matrix $\boldsymbol{G}$ and the M-vector $\boldsymbol{K}(\boldsymbol{z})$ are given by

$$\boldsymbol{G} = \begin{bmatrix} 2 & -1 & 0 & \cdots & 0 \\ -1 & 2 & -1 & \ddots & \vdots \\ 0 & \ddots & \ddots & \ddots & 0 \\ \vdots & \ddots & -1 & 2 & -1 \\ 0 & \cdots & 0 & -1 & 2 \end{bmatrix}, \quad \boldsymbol{K}(\boldsymbol{z}) = \beta \begin{pmatrix} K(z_1) \\ K(z_2) \\ \vdots \\ K(z_M) \end{pmatrix}, \quad \beta = \frac{\mu}{\Delta x^2}.$$

Let $\boldsymbol{E}(\boldsymbol{z}) = \beta \operatorname{diag}(L(z_1), \dots, L(z_M))$, then $\boldsymbol{K}(\boldsymbol{z}) = \boldsymbol{E}(\boldsymbol{z})\boldsymbol{z}$. Assume that $\boldsymbol{z} \geq \boldsymbol{0}$. Then $\boldsymbol{I} + \boldsymbol{G}\boldsymbol{E}(\boldsymbol{z})$ is a strictly diagonally dominant matrix with positive diagonal entries and non-positive off-diagonal entries, and therefore $(\boldsymbol{I} + \boldsymbol{G}\boldsymbol{E}(\boldsymbol{z}))^{-1}$ is a nonnegative matrix and it is a continuous function of $\boldsymbol{z}$. Then, the solution of equation (2.19) is reduced to finding fixed points of the mapping

$$\boldsymbol{z} \mapsto \boldsymbol{\varphi}(\boldsymbol{z}) = \big(\boldsymbol{I} + \boldsymbol{G}\boldsymbol{E}(\boldsymbol{z})\big)^{-1} \boldsymbol{c}.$$

To assess existence of fixed points, we aim to apply Brouwer's theorem to $\boldsymbol{\varphi}$ and the compact and convex set $\mathcal{K} := \{\boldsymbol{z} \in \mathbb{R}^M \mid \boldsymbol{z} \geq \boldsymbol{0} \text{ and } \|\boldsymbol{z}\|_1 \leq \|\boldsymbol{c}\|_1\}$. Clearly, $(\boldsymbol{I} + \boldsymbol{G}\boldsymbol{E}(\boldsymbol{z}))^{-1} \geq \boldsymbol{0}$ and $\boldsymbol{c} \geq \boldsymbol{0}$ immediately yield $\boldsymbol{\varphi}(\boldsymbol{z}) \geq \boldsymbol{0}$ for all $\boldsymbol{z} \in \mathcal{K}$, so, to prove that $\boldsymbol{\varphi}(\mathcal{K}) \subseteq \mathcal{K}$, there only remains to prove that

$$\big\|\boldsymbol{\varphi}(\boldsymbol{z})\big\|_1 \leq \|\boldsymbol{c}\|_1 \quad \text{for all } \boldsymbol{z} \in \mathcal{K}. \tag{2.20}$$

To this end, we take into account that

$$\big\|\boldsymbol{\varphi}(\boldsymbol{z})\big\|_1 \leq \big\|\big(\boldsymbol{I} + \boldsymbol{G}\boldsymbol{E}(\boldsymbol{z})\big)^{-1}\big\|_1 \|\boldsymbol{c}\|_1.$$

Thus, to establish (2.20) it is sufficient to prove that

$$\big\|\big(\boldsymbol{I} + \boldsymbol{G}\boldsymbol{E}(\boldsymbol{z})\big)^{-1}\big\|_1 \leq 1 \quad \text{for all } \boldsymbol{z} \in \mathcal{K}.$$

For this purpose, we use the auxiliary matrix

$$\tilde{\boldsymbol{G}} := \begin{bmatrix} 1 & -1 & 0 & \cdots & 0 \\ -1 & 2 & -1 & \ddots & \vdots \\ 0 & \ddots & \ddots & \ddots & 0 \\ \vdots & \ddots & -1 & 2 & -1 \\ 0 & \cdots & 0 & -1 & 1 \end{bmatrix}$$

and the notation $\boldsymbol{H} := \boldsymbol{I}+\boldsymbol{G}\boldsymbol{E}(\boldsymbol{z})$ and $\boldsymbol{M} := \boldsymbol{I} + \tilde{\boldsymbol{G}}\boldsymbol{E}(\boldsymbol{z})$. The same previous argument yields that $\boldsymbol{M}^{-1} \geq \boldsymbol{0}$. Now, for $\boldsymbol{e} := (1, \dots, 1)^{\mathrm{T}} \in \mathbb{R}^M$ it follows that $\boldsymbol{e}^{\mathrm{T}}\tilde{\boldsymbol{G}} = \boldsymbol{0}$, so $\boldsymbol{e}^{\mathrm{T}}\boldsymbol{M} = \boldsymbol{e}^{\mathrm{T}}$ and $\boldsymbol{e}^{\mathrm{T}}\boldsymbol{M}^{-1} = \boldsymbol{e}^{\mathrm{T}}$. If we assume that $\boldsymbol{H}^{-1} = (\bar{\eta}_{ij})_{1\leq i,j\leq M}$ and $\boldsymbol{M}^{-1} = (\bar{\mu}_{ij})_{1\leq i,j\leq M}$, then this is equivalent to

$$\sum_{i=1}^{M} \bar{\mu}_{ij} = 1, \quad j = 1, \dots, M.$$

Furthermore, since $\boldsymbol{H}^{-1} \geq \boldsymbol{0}$, $\boldsymbol{M}^{-1} \geq \boldsymbol{0}$ and $\boldsymbol{H} - \boldsymbol{M} = \beta \operatorname{diag}(L(z_1), 0, \dots, 0, L(z_M)) \geq \boldsymbol{0}$ for $\boldsymbol{z} \in \mathcal{K}$ and

$$\boldsymbol{H}^{-1} = \boldsymbol{M}^{-1} - \boldsymbol{H}^{-1}(\boldsymbol{H} - \boldsymbol{M})\boldsymbol{M}^{-1},$$

it follows that $\boldsymbol{H}^{-1} \leq \boldsymbol{M}^{-1}$. This yields that

$$\|\boldsymbol{H}^{-1}\|_1 = \max_{1\leq j\leq M} \sum_{i=1}^{M} \bar{\eta}_{ij} \leq \max_{1\leq j\leq M} \sum_{i=1}^{M} \bar{\mu}_{ij} = 1.$$

Applying Brouwer's fixed point theorem to the continuous function $\boldsymbol{\varphi}\colon \mathcal{K} \to \mathcal{K}$ we deduce the existence of a fixed point of $\boldsymbol{\varphi}$, i.e. a nonnegative solution to equation (2.18).

For uniqueness, we adapt an argument that can be found in [34] and define

$$\Psi(\boldsymbol{z}) := \beta \sum_{i=1}^{M} N\big(|z_i|\big),$$

where N is a primitive of K, and

$$f(\boldsymbol{z}) := \frac{1}{2}\boldsymbol{z}^{\mathrm{T}}\boldsymbol{A}^{-1}\boldsymbol{z} + \Psi(\boldsymbol{z}) - \boldsymbol{z}^{\mathrm{T}}\boldsymbol{A}^{-1}\boldsymbol{c}.$$

Since $K(0) = K'(0) = 0$, Ψ is twice continuously differentiable. Therefore f is also twice continuously differentiable and its gradient $f'(\boldsymbol{z})$ and Hessian $f''(\boldsymbol{z})$ are given by the respective expressions

$$f'(\boldsymbol{z})^{\mathrm{T}} = \boldsymbol{A}^{-1}\boldsymbol{z} + \beta \begin{pmatrix} \operatorname{sgn}(z_1)K(|z_1|) \\ \vdots \\ \operatorname{sgn}(z_M)K(|z_M|) \end{pmatrix} - \boldsymbol{A}^{-1}\boldsymbol{c}, \quad f''(\boldsymbol{z}) = \boldsymbol{A}^{-1} + \beta \operatorname{diag}\big(K'(|z_1|), \dots, K'(|z_M|)\big).$$

Since $\boldsymbol{A}^{-1}$ is symmetric and positive definite and $\beta K'(|z_i|) \geq 0$, it follows that $f''(\boldsymbol{z})$ is symmetric and positive definite, therefore f is strictly convex, so any critical point (at which $f'(\boldsymbol{z}) = \boldsymbol{0}$) is the unique global minimum. Now, if $\boldsymbol{z} + \boldsymbol{A}\boldsymbol{K}(\boldsymbol{z}) = \boldsymbol{c}$ with $\boldsymbol{z} \geq \boldsymbol{0}$, then $f'(\boldsymbol{z}) = \boldsymbol{0}$ and $\boldsymbol{z} \in \mathcal{K}$, so positive solutions of (2.19) are critical points of f, so uniqueness is proven. □

Theorem 2.3. *If K satisfies the conditions* (2.3)*, the quantities $u_{j+1/2}$ in* (2.10) *satisfy $u_{j+1/2} \geq 0$ for $j = 1, \dots, M-1$ and*

$$\frac{\Delta t}{\Delta x} \max_j |v_{j+1/2}| \leq 1/2 \tag{2.21}$$

then the Euler IMEX method

$$\boldsymbol{u}^{n+1} = \boldsymbol{u}^n + \Delta t\big(\boldsymbol{\mathcal{C}}(\boldsymbol{u}^n) + \boldsymbol{\mathcal{D}}(\boldsymbol{u}^{n+1})\big)$$

is a positivity preserving scheme.

Proof. Let $\boldsymbol{b}^n := \boldsymbol{u}^n + \Delta t\boldsymbol{\mathcal{C}}(\boldsymbol{u}^n)$. Then it follows from Theorem 2.1 with $K = 0$ that $\boldsymbol{b}^n \geq \boldsymbol{0}$. Since the equation $\boldsymbol{u}^{n+1} = \boldsymbol{b}^n + \Delta t\boldsymbol{\mathcal{D}}(\boldsymbol{u}^{n+1})$ can be rewritten as $\boldsymbol{z} - \Delta t\boldsymbol{\mathcal{D}}(\boldsymbol{z}) = \boldsymbol{c}$ for $\boldsymbol{z} = \boldsymbol{u}^{n+1}$, $\boldsymbol{c} = \boldsymbol{b}^n$, Theorem 2.2 yields that a unique nonnegative solution $\boldsymbol{z}$ exists. This concludes the proof. □

Unfortunately, this result cannot be directly applied to higher-order RK-IMEX schemes, since there cannot be Runge-Kutta implicit schemes in SSP form of order higher than one (see [33]), so Theorem 2.2 cannot be in principle applied for second-order accuracy in time. We have nevertheless used Newton-Raphson method, together with a line search algorithm (see [28]) to solve (2.16). At each step of this algorithm a tridiagonal

system is solved. We have not experienced any troubles in solving these systems under a stability restriction as (2.21).

3. Numerical results

3.1. **Preliminaries.** In the following examples, we solve (1.3) numerically for $0 \le t \le T$ and $-L \le x \le L$. We compare numerical results obtained by the IMEX-RK scheme proposed herein with those obtained by the explicit scheme of [1]. For each time step $\Delta t = \Delta t_n$ is determined by the formula

$$\frac{\Delta t}{\Delta x}\max_j\big|v^n_{j+1/2}\big| + \frac{\Delta t}{\Delta x^2}\max_u\big|K'(u)\big| = C_{\mathrm{cfl}_1} \tag{3.1}$$

for the explicit scheme and by

$$\frac{\Delta t}{\Delta x}\max_j\big|v^n_{j+1/2}\big| = C_{\mathrm{cfl}_2} \tag{3.2}$$

for the IMEX-RK scheme. In the numerical examples we choose C_{cfl_1} and C_{cfl_2} in the respective cases as the largest multiple of 0.05 that yields oscillation-free reference solutions.

For comparison purposes, we compute reference solutions for numerical tests with $M_{\mathrm{ref}} = 12800$ cells with the IMEX-RK scheme for Examples 1, 2, and 3, and with the first-order scheme of [10] for Example 4 (see Section 3.4 for a description of that scheme). We compute approximate L^1 errors at different times for each scheme as follows. We denote by $(u^M_j(t))_{j=1}^M$ and $(u^{\mathrm{ref}}_j(t))_{j=1}^{M_{\mathrm{ref}}}$ the numerical solution at time t calculated with M and M_{ref} cells, respectively. We assume that $R := M_{\mathrm{ref}}/M$ is an integer and compute the projection of the reference solution $\tilde{u}^{\mathrm{ref},M}_j(t)$, $j = 1, \ldots, M$, by

$$\tilde{u}^{\mathrm{ref},M}_j(t) = \frac{1}{R}\sum_{k=1}^{\mathrm{R}} u^{\mathrm{ref}}_{R(j-1)+k}(t).$$

The approximate L^1 error $e_M(t)$ associated with the numerical solution on the mesh with M cells at time t is then given by

$$e_M(t) := \frac{1}{M}\sum_{j=1}^{M}\big|\tilde{u}^{\mathrm{ref},M}_j(t) - u^M_j(t)\big|.$$

A numerical order of convergence can be calculated from pairs $e_{M/2}(t)$ and $e_M(t)$ by

$$\theta_M(t) := \log_2\big(e_M(t)/e_{2M}(t)\big).$$

In our simulations we limit ourselves to the second-order IMEX-RK scheme defined by

$$\boldsymbol{D} := \begin{array}{c|cc} 1/2 & 1/2 & 0 \\ 1/2 & 0 & 1/2 \\ \hline & 1/2 & 1/2 \end{array}, \quad \tilde{\boldsymbol{D}} := \begin{array}{c|cc} 0 & 0 & 0 \\ 1 & 1 & 0 \\ \hline & 1/2 & 1/2 \end{array}.$$

3.2. **Examples 1 and 2.** In Examples 1 and 2 we consider the numerical experiment proposed in [1] to simulate and compare the numerical solution of (1.3). Example 1 corresponds to equation (1.3) where the initial condition u_0 along with the functions W and H respectively are given by

$$u_0(x) = \frac{1}{\sqrt{8\pi}}\big(\exp(-0.5(x-3)^2) + \exp(-0.5(x+3)^2)\big), \quad W(x) = \frac{1}{\sqrt{2\pi\sigma}}\exp\left(-\frac{|x|^2}{2\sigma}\right), \quad H(u) = \frac{\nu}{m}\,u^m.$$

In Example 1 we consider the pairs $(m, \nu) = (1.5, 0.33)$, $(2, 0.48)$, and $(3, 2.6)$ that cover the cases $0 < m < 2$, $m = 2$, and $m > 2$, respectively. The corresponding functions $K'(u)$, that is the nonlinear diffusion coefficients, for these three cases are plotted in Figure 1. The simulations are run on the computational domain $[-L, L] = [-10, 10]$. Numerical solutions for the final times $T = 250$ and $T = 1250$ for each of the three parameter choices, and obtained with a relatively coarse discretization of $M = 200$ subintervals, are shown in Figure 2. Table 1 displays the approximate L^1 errors, corresponding convergence rates, and CPU times for each of these pairs of parameters for a number of final times and successive discretizations. The

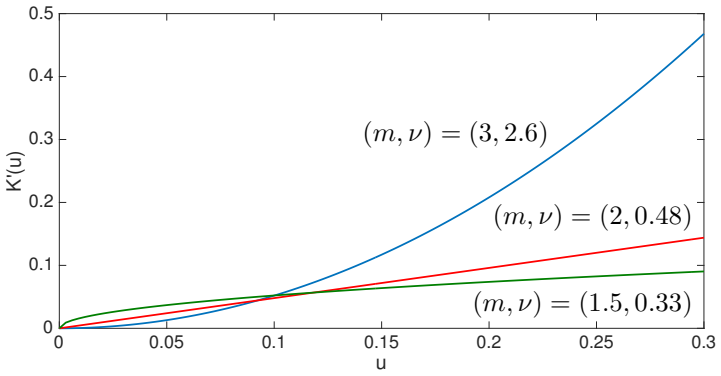

FIGURE 1. Example 1: nonlinear diffusion functions $K'(u) = uH''(u)$ for $H(u) = (\nu/m)u^m$ for the indicated pairs (m, ν).

information of Table 1 is plotted in Figure 3 in terms of efficiency, that is, in terms of reduction of numerical error versus CPU time.

First of all, we observe that for $(m, \nu) = (1.5, 0.33)$, the reference solution is smooth while for $(m, \nu) = (2, 0.48)$ and $(3, 2.6)$, the solution has "kinks" at the basis of the "peak" that is forming. Moreover, we observe that the numerical errors produced by both the IMEX-RK and the explicit schemes roughly reduce at an observed second-order rate of convergence, which is also the theoretical order of accuracy (both in space and time). For a given discretization M, the explicit scheme produces significantly smaller approximate errors than the corresponding IMEX-RK scheme for the cases $(m, \nu) = (1.5, 0.33)$ and $(m, \nu) = (2, 0.48)$, while for $(m, \nu) = (3, 2.6)$ and $M \geq 400$ the error produced by the IMEX-RK scheme are smaller than those of the explicit scheme. While the results do not favor one or the other scheme in terms of accuracy, CPU times for the IMEX-RK scheme are substantially smaller than for the explicit scheme. This observation gives rise to the question of efficiency, that is to which of the schemes turns out to be more efficient in terms of reduction of error per CPU time. Figure 3 indicates that for $(m, \nu) = (1.5, 0.33)$ and $(m, \nu) = (2, 0.48)$ the explicit scheme is most efficient for $M \leq 800$ but gained by the IMEX-RK scheme, while for $(m, \nu) = (3, 2.6)$, the IMEX-RK scheme is most efficient in almost all instances. In fact, in light of Figure 1 and the range of solution values attained the third case is the one that involves the highest values of $K'(u)$, that is where diffusion is most dominant and therefore the gain in efficiency by using an IMEX-RK scheme instead of a comparable explicit scheme is most significant. Related findings have been obtained for systems of convection-diffusion equations modeling equilibrium chromatography [29].

In Example 2 we consider the same function H as in Example 1 but now choose $m = 3$ and $\nu = 1.48$. The functions W and u_0 are given by

$$W(x) = \begin{cases} 1 - |x| & \text{if } |x| \leq 1, \\ 0 & \text{otherwise,} \end{cases} \qquad u_0(x) = \begin{cases} 0.05 & \text{if } x \in [-3, 3], \\ 0 & \text{otherwise.} \end{cases}$$

The numerical simulation are run over the computational domain $[-6, 6]$ until final time $T = 105$. Numerical results at $T = 0$ (the initial condition), $T = 45$, $T = 75$ and $T = 105$ are shown in Figure 4. Table 2 provides the corresponding approximate L^1 errors, convergence rates, and CPU times, and Figure 5 shows the efficiency plots for $T = 45$ and $T = 75$. First of all, it is interesting to note that the model predicts that one initial block of "mass" is split into three separate portions of which the middle one disappears later and two portions remain. For this model, the IMEX-RK scheme produces slightly larger errors but is considerably faster than the explicit scheme, and therefore turns out significantly more efficient (see Figure 5).

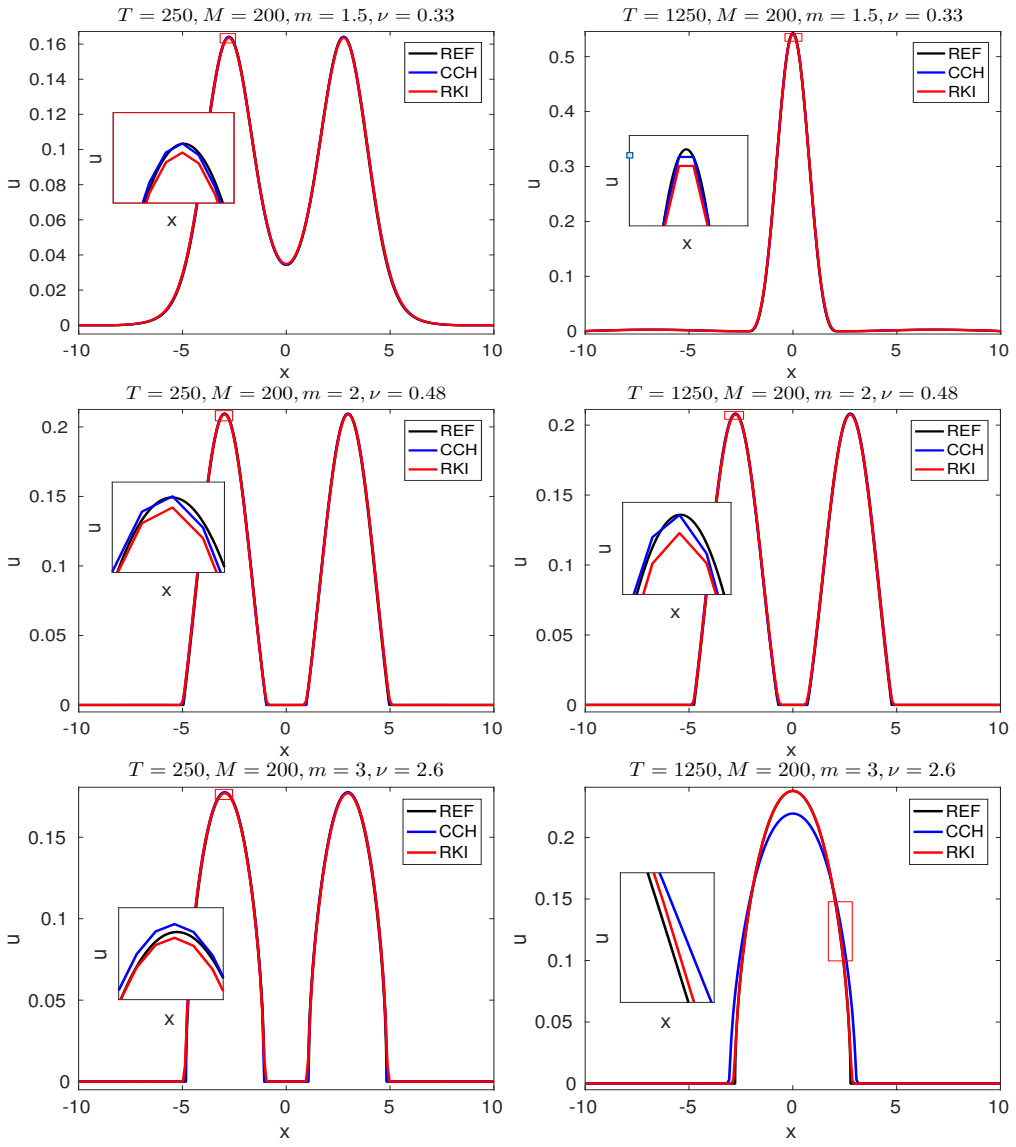

FIGURE 2. Example 1: numerical solutions with $\Delta x = 2L/M$, $L = 10$ and $M = 200$ for (top) $m = 1.5$, $\nu = 0.33$, (middle) $m = 2$, $\nu = 0.48$, (bottom) $m = 3$, $\nu = 2.6$ at simulated time (left) $T = 250$, (right) $T = 1250$.

3.3. **Example 3.** This example represents a slight modification of Example 1, namely we choose W and H as in Example 1, but we utilize the initial function

$$u_0(x) = \frac{1}{\sqrt{8\pi}}\big(\exp(-0.2(x+7)^2) + \exp(-0.2x^2) + \exp(-0.2(x-7)^2)\big).$$

Moreover, we consider the pairs of parameter values $(m, \nu) = (3, 2.6)$ and $(m, \nu) = (3, 3)$ and with a CFL condition (3.1) with $C_{\mathrm{cfl}_1} = 0.5$ for the explicit scheme. The numerical results are displayed in Figures 6 and 7, the approximate errors, convergence rates and CPU times are provided in Table 3, and Figure 8 contains the efficiency plots for two of the six end times T for which the errors are measured. According to Table 3, for $(m, \nu) = (3, 2.6)$ the IMEX-RK produces smaller errors (for $M \geq 200$) and occupies less CPU

		IMEX-RK			Explicit			IMEX-RK			Explicit		
	M	e_M	θ_M	cpu [s]	e_M	θ_M	cpu [s]	e_M	θ_M	cpu [s]	e_M	θ_M	cpu [s]
$m = 1.5$,		$T = 250$						$T = 1000$					
$\nu = 0.33$	100	813.43	—	0.02	90.11	—	0.02	672.99	—	0.14	166.74	—	0.10
	200	200.03	2.02	0.12	22.94	1.97	0.11	174.22	1.95	0.69	42.00	1.99	0.60
	400	49.15	2.03	0.41	5.82	1.98	1.34	46.98	1.89	3.05	10.84	1.95	7.18
	800	12.12	2.02	1.93	1.49	1.96	11.96	13.13	1.84	14.25	2.71	2.00	65.57
	1600	2.98	2.03	8.59	0.41	1.88	103.98	3.88	1.76	64.94	0.73	1.89	562.33
		$T = 1250$						$T = 1500$					
	100	664.34	—	0.20	166.36	—	0.12	654.96	—	0.24	165.64	—	0.15
	200	174.50	1.93	0.93	41.93	1.99	0.80	174.39	1.91	1.16	41.73	1.99	1.01
	400	47.18	1.89	4.25	10.87	1.95	9.53	46.60	1.90	5.46	10.72	1.96	11.88
	800	13.48	1.81	19.85	2.71	2.00	87.38	13.32	1.81	25.50	2.70	1.99	109.32
	1600	4.10	1.72	90.79	0.75	1.86	746.51	4.05	1.72	116.89	0.75	1.85	930.66
$m = 2$,		$T = 250$						$T = 1000$					
$\nu = 0.48$	100	550.43	—	0.02	52.32	—	0.03	1326.63	—	0.08	170.40	—	0.10
	200	125.23	2.14	0.08	53.62	-0.04	0.12	291.96	2.18	0.32	81.76	1.06	0.44
	400	33.27	1.91	0.43	4.79	3.49	1.58	69.68	2.07	1.74	7.54	3.44	6.18
	800	7.82	2.09	2.11	2.78	0.78	14.43	17.06	2.03	8.42	5.36	0.49	58.24
	1600	1.91	2.03	9.47	0.51	2.44	125.89	4.10	2.06	38.53	1.01	2.41	507.48
		$T = 1250$						$T = 1500$					
	100	2440.04	—	0.10	351.76	—	0.12	9490.83	—	0.13	900.67	—	0.13
	200	503.08	2.38	0.40	139.83	1.33	0.55	1353.28	2.81	0.48	295.33	1.61	0.65
	400	123.00	2.03	2.18	8.43	4.05	7.71	308.88	2.13	2.67	23.82	3.63	9.23
	800	29.57	2.06	10.52	8.07	0.06	72.78	74.10	2.06	12.60	16.97	0.49	87.23
	1600	7.08	2.06	48.32	1.71	2.24	634.09	17.69	2.07	58.52	4.16	2.03	759.88
$m = 3$,		$T = 250$						$T = 1000$					
$\nu = 2.6$	100	760.70	—	0.03	878.66	—	0.03	6169.47	—	0.11	3103.46	—	0.11
	200	205.09	1.89	0.09	265.34	1.73	0.23	534.51	3.53	0.39	2630.90	0.24	0.75
	400	84.90	1.27	0.48	147.96	0.84	2.48	100.05	2.42	1.92	1491.90	0.82	9.93
	800	27.88	1.61	2.23	32.92	2.17	23.91	25.66	1.96	8.92	431.48	1.79	95.54
	1600	8.31	1.75	10.07	10.62	1.63	204.71	12.86	1.00	40.69	102.78	2.07	818.11
		$T = 1250$						$T = 1500$					
	100	280.86	—	0.13	7868.90	—	0.13	437.82	—	0.15	239.35	—	0.16
	200	113.89	1.30	0.49	4804.94	0.71	0.91	146.85	1.58	0.61	72.66	1.72	1.21
	400	46.04	1.31	2.44	1052.02	2.19	12.27	40.12	1.87	3.04	54.92	0.40	16.67
	800	14.58	1.66	11.41	149.30	2.82	119.93	17.51	1.20	14.23	11.10	2.31	163.30
	1600	5.19	1.49	51.99	29.97	2.32	1040.56	5.20	1.75	64.76	9.93	0.16	1413.58

TABLE 1. Example 1: approximate L^1 errors (e_M, figures to be multiplied by 10^{-6}), convergence rates (θ_M), and CPU times (cpu).

time than the explicit scheme, while for $(m, \nu) = (3, 3)$ the same happens for sufficiently fine discretizations. Summarizing, we can say that according to Table 3 for $M \geq 400$ (but in many runs even for coarser discretizations) the IMEX-RK scheme is more efficient than the explicit version.

3.4. **Example 4.** In this example we come back to the one-dimensional aggregation model outlined in Section 1.2, and present a numerical example of (1.3), (1.4) that is also a solution to the aggregation

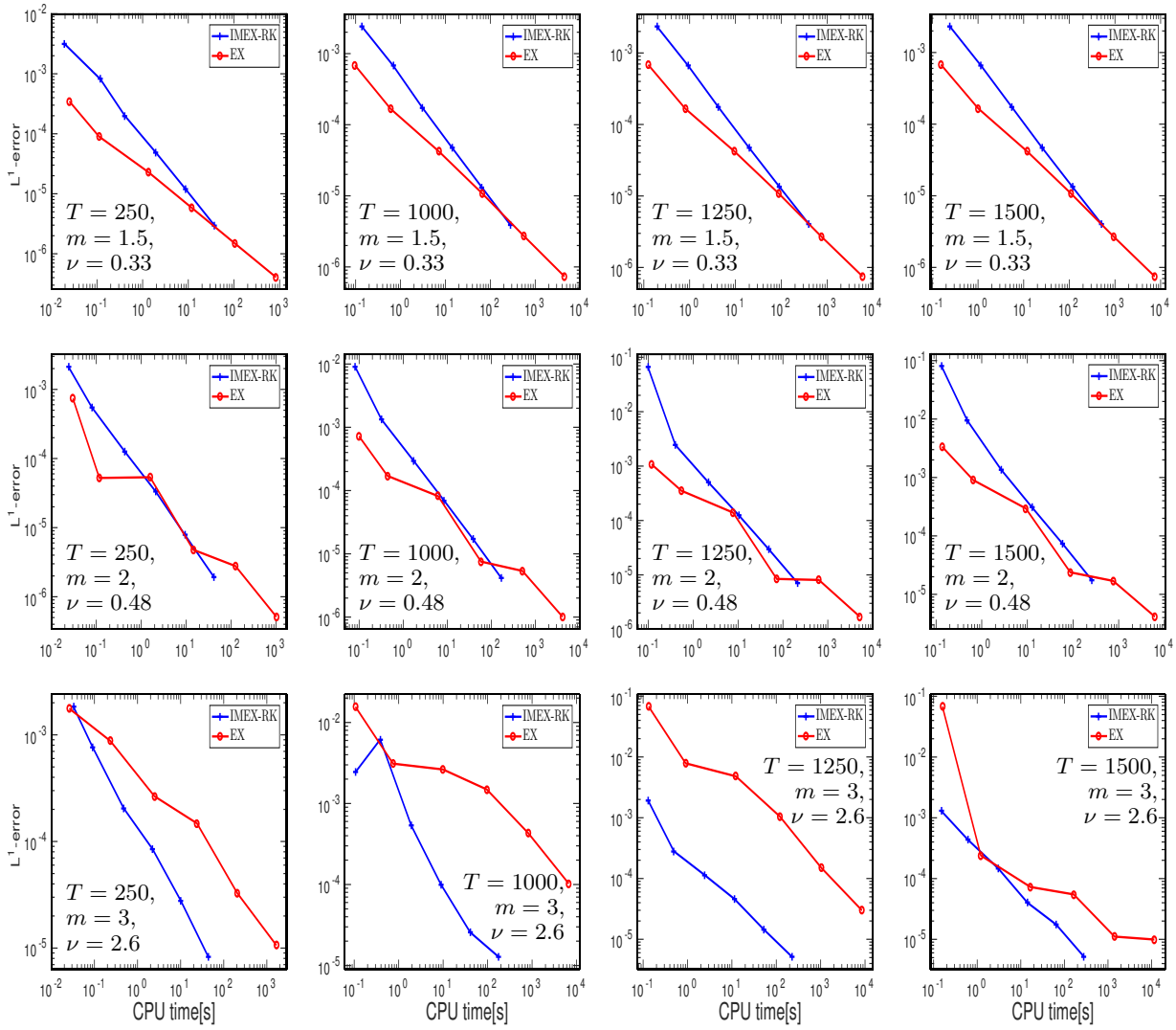

FIGURE 3. Example 1: efficiency plots: approximate L^1 errors versus CPU times for three pairs (m, ν), corresponding to four simulated times.

equation (1.5). We consider the numerical experiment proposed in [10], and first specify the initial condition

$$u_0(x) = \begin{cases} 5 & \text{for } 0.1 \le x \le 0.2, \\ 8 & \text{for } 0.6 \le x \le 0.7, \\ 7 & \text{for } 0.8 \le x \le 0.9, \\ 0 & \text{otherwise,} \end{cases}$$

such that $C_0 = 2$. Then we set $\Phi(q) = -(1-q)^2$, which ensures that (1.7) recovers (1.5) (with $k = 1$), and correspondingly, $W(x) = |x|$. Moreover, the numerical experiment of [10] stipulates the strongly degenerating diffusion function

$$a(u) = \begin{cases} 0 & \text{for } u \le u_c, \\ a_0 & \text{for } u > u_c, \end{cases}$$

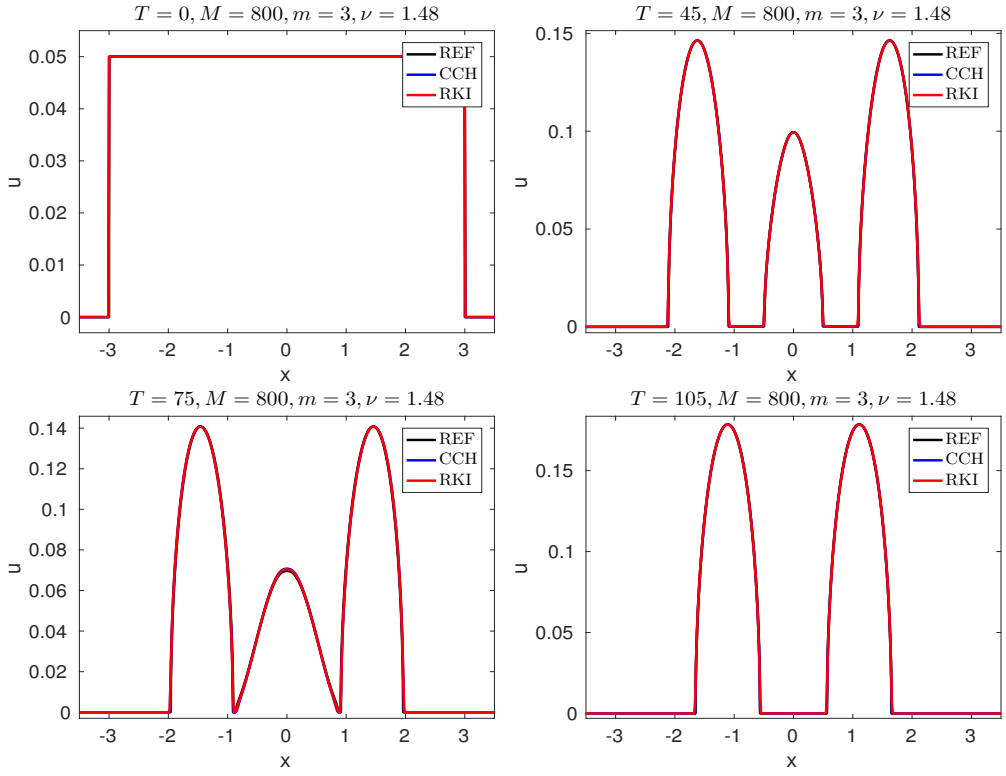

FIGURE 4. Example 2: numerical solution for $m = 3, \nu = 1.48$, $\Delta x = 2L/M$ with $L = 6$ and $M = 800$.

	IMEX-RK			Explicit			IMEX-RK			Explicit		
M	e_M	θ_M	cpu [s]	e_M	θ_M	cpu [s]	e_M	θ_M	cpu [s]	e_M	θ_M	cpu [s]
	$T = 30$						$T = 45$					
100	969.59	—	0.03	488.36	—	0.03	1080.25	—	0.04	927.04	—	0.05
200	323.50	1.58	0.14	150.69	1.70	0.40	337.41	1.68	0.23	398.01	1.22	0.74
400	101.33	1.67	0.65	71.40	1.08	3.50	142.30	1.25	1.08	133.36	1.58	6.58
800	30.74	1.72	2.94	25.67	1.48	29.96	63.65	1.16	4.89	36.11	1.88	56.38
1600	10.91	1.49	12.40	7.01	1.87	250.92	23.69	1.43	20.63	14.33	1.33	472.33
	$T = 75$						$T = 105$					
100	2504.19	—	0.08	5528.90	—	0.11	1922.98	—	0.12	1343.35	—	0.17
200	456.17	4.46	0.42	2429.61	1.19	1.40	688.71	1.48	0.63	679.48	0.98	2.20
400	472.92	-0.05	1.95	952.62	1.35	12.61	210.39	1.71	2.91	100.70	2.75	20.20
800	245.74	0.94	8.78	337.33	1.50	108.16	71.85	1.55	13.15	66.79	0.59	174.81
1600	99.88	1.30	37.35	117.18	1.53	903.16	20.34	1.82	56.10	7.02	3.25	1495.84

TABLE 2. Example 2: approximate L^1 errors (e_M, figures to be multiplied by 10^{-6}), convergence rates (θ_M), and CPU times (cpu) for $m = 3$ and $\nu = 1.48$.

where $a_0 = 0.1$ and $u_c = 10$ is a critical density value.

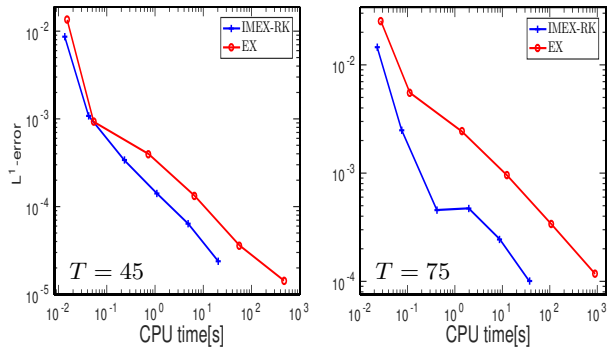

FIGURE 5. Example 2: efficiency plots based on numerical solutions for $\Delta x = 2L/M$, with $L = 6$ and $M = 100, 200, 400, 800$ and 1600.

The numerical scheme for the initial value problem (1.8), analyzed in [10] and which is utilized in this example to calculate the reference solution, is defined as follows. We first set

$$q_j^0 := q_0(x_j) = \int_{-M}^{x_j} u_0(x)\,\mathrm{d}x, \tag{3.3}$$

and then utilize the explicit marching formula

$$\begin{aligned} q_j^{n+1} = q_j^n - \frac{\Delta t}{\Delta x}\Bigg[& \big(h(q_j^n, q_{j-1}^n) - h(q_{j-1}^n, q_j^n)\big) \\ & - \left(A\left(\frac{q_{j+1}^n - q_j^n}{\Delta x}\right) - A\left(\frac{q_j^n - q_{j-1}^n}{\Delta x}\right)\right)\Bigg], \quad j = 1, \ldots, M, \quad n \in \mathbb{N}_0, \end{aligned} \tag{3.4}$$

where Δt and Δx are subject to the CFL condition

$$\frac{\Delta t}{\Delta x} \max_{q\in[0,C_0]} \big|\Phi'(q)\big| + \frac{\Delta t}{\Delta x^2} \max_{u\in\mathbb{R}} \big|a(u)\big| \leq \frac{1}{2}, \tag{3.5}$$

and h is the Engquist-Osher flux [35], a monotone numerical flux [36] consistent with Φ that is given by

$$h(q, r) = \Phi(0) + \int_0^q \max\big\{0, \Phi'(s)\big\}\,\mathrm{d}s + \int_0^r \min\big\{0, \Phi'(s)\big\}\,\mathrm{d}s.$$

To recover u from the numerical solution of (1.8) we use the divided difference $u_j^n = (q_{j+1}^n - q_j^n)/\Delta x$ which gives a numerical method for equation (1.7) that provably converges as $\Delta t \to 0$ to the unique entropy solution of (1.7), (1.4) [10]. Here we employ the aforementioned scheme with $M_{\mathrm{ref}} = 12800$ to calculate a reference solution to compare the performances of the IMEX-RK and explicit schemes.

Numerical results are shown in Figure 9. The approximate errors, convergence rates and CPU times are displayed in Table 4, and Figure 10 contains the corresponding efficiency plots. The results of Figure 9 alert to the fact that solutions of this model are in general discontinuous due to the strongly degenerate nature of the diffusion and the imposition of discontinuous initial data. In this case the ingredients of the equation have been designed such that all "mass" ("animals") move to the center of mass and eventually form one single group ("herd"). We observe slight "kinks" in the solution profiles near $u = u_c = 10$. Above this value of density the repulsive effect of degenerate diffusion sets on, and it is precisely this effect which prevents the model from forming unbounded densities (at least, in finite time [10]). On the other hand, it is well known that in the presence of discontinuities the observed order of convergence is much lower than its formal (in this case, second) order of accuracy, as can bee seen in Table 4. Nevertheless, it appears that both the solution of the IMEX-RK and the explicit scheme converge to the reference solution produced by (3.3), (3.4), and the IMEX-RK occupies only a fraction of the CPU time in comparison with the explicit scheme (for instance, less than 1% for $M = 1600$), and therefore turns out more efficient than the explicit scheme, as is reconfirmed by Figure 10.

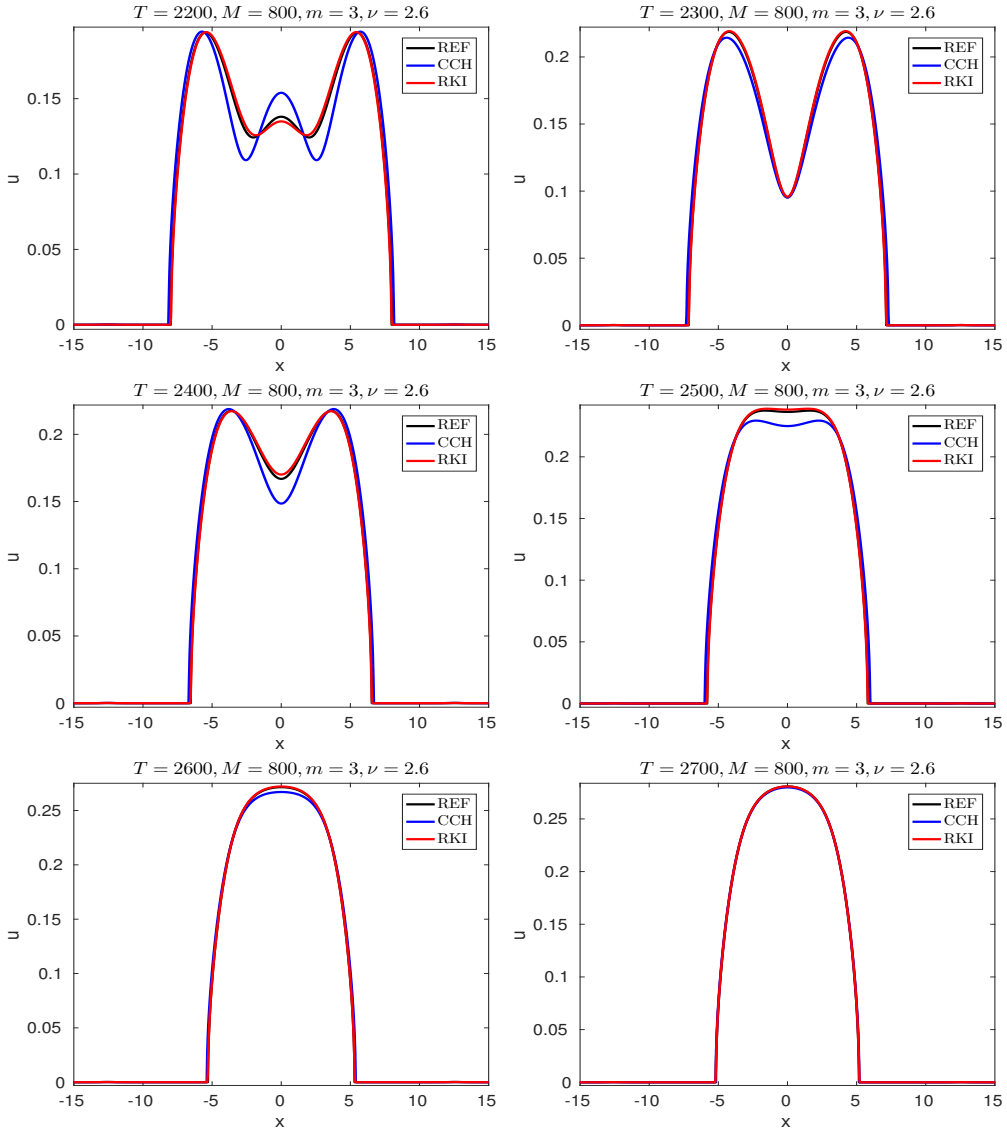

FIGURE 6. Example 3: numerical solution for $m = 3$, $\nu = 2.6$, $\Delta x = 2L/M$ with $L = 15$, and $M = 800$.

4. Conclusions

We have shown that a particular IMEX-RK scheme represents a serious alternative to the explicit scheme introduced in [1] for the efficient numerical solution of the one-dimensional nonlinear nonlocal equation (1.3). At a fixed spatial discretization the explicit scheme is more accurate in most settings. However, the gain in CPU time (due to the less restrictive CFL condition) by the IMEX-RK scheme is in most circumstances, and in particular for fine discretizations, so significant that the IMEX-RK scheme turns out most efficient in terms of error reduction per CPU time. In this respect we mention that higher-order IMEX-RK schemes have also been tested, but with less significant gains of accuracy at least for the moderately fine discretizations used in this work. Of course, the gain of efficiency attainable by an IMEX-RK scheme depends on the relative magnitude of the diffusion versus convection terms, a parameter that we did not vary herein since

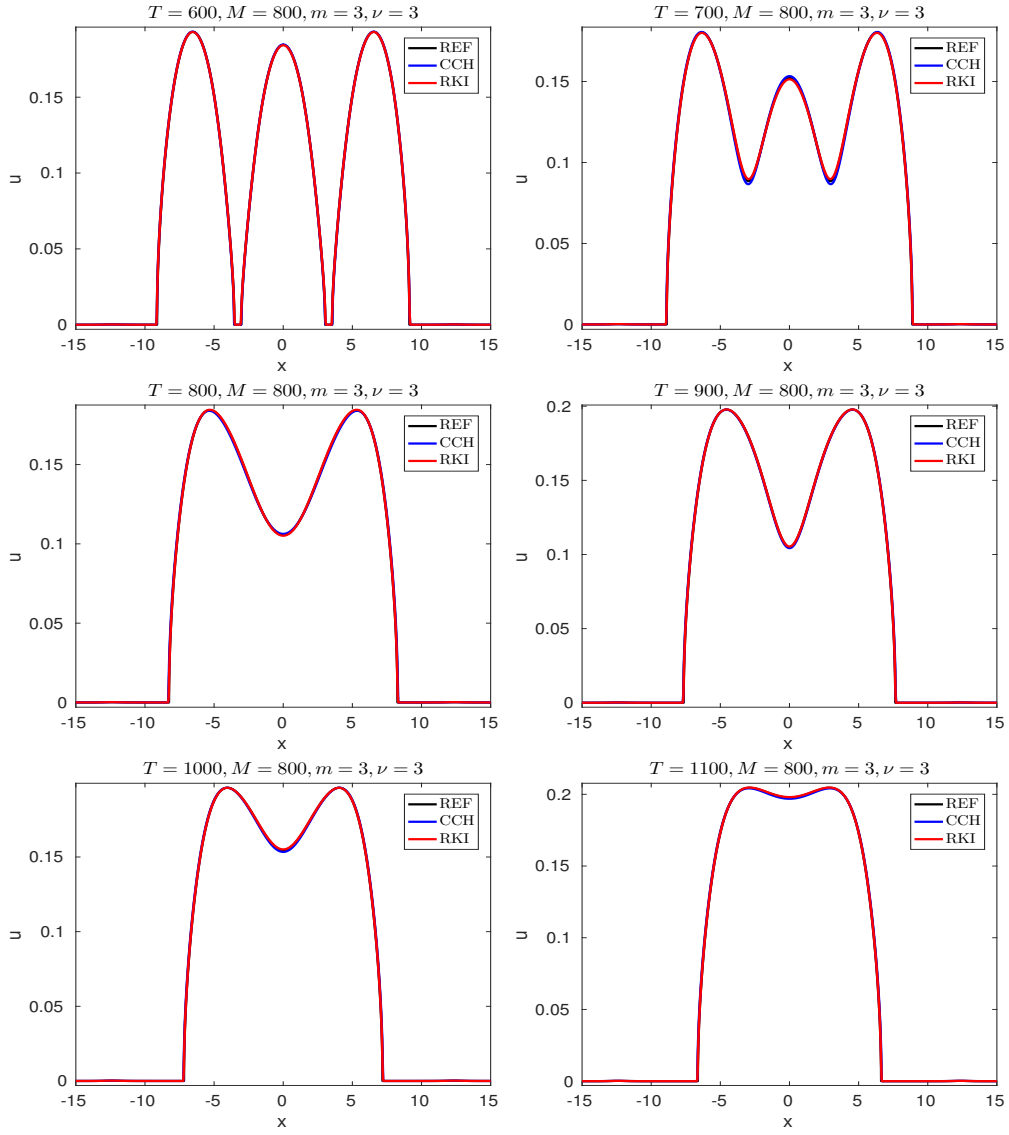

FIGURE 7. Example 3: numerical solution for $m = 3$, $\nu = 3$, $\Delta x = 2L/M$ with $L = 15$, and $M = 800$.

we insist on adopting the test cases of [1] (Examples 1 to 3) and [10] (Example 4). Future research will furthermore address the case of two or three space dimensions, for which the extension of the IMEX-RK approach is straightforward (apart from the more involved structure of the algebraic systems to be solved). That said, we mention that the scenario of Example 4, and in particular the convenient computation of a reference solution by solving a local PDE, does not have a counterpart in two or three space dimensions since the aggregation model, outlined in Section 1.2, cannot be extended in a straightforward way to several dimensions. This observation has been our prime motivation to analyze the one-dimensional case separately.

ACKNOWLEDGMENTS

RB is supported by Fondecyt project 1170473 and CRHIAM, Proyecto Conicyt Fondap 15130015. DI acknowledges CONICYT scholarship CONICYT-PCHA/Doctorado Nacional/2014-21140362. PM is supported

		IMEX-RK			Explicit			IMEX-RK			Explicit		
	M	e_M	θ_M	cpu [s]	e_M	θ_M	cpu [s]	e_M	θ_M	cpu [s]	e_M	θ_M	cpu [s]
$m=3$,		$T=2000$						$T=2200$					
$\nu=2.6$	100	25373.15	—	0.38	21792.46	—	0.63	28245.49	—	0.42	55270.59	—	0.70
	200	4019.83	2.66	2.00	21466.65	0.02	8.83	16656.50	0.76	2.21	55102.84	0.00	9.67
	400	1013.94	1.99	9.86	2628.76	3.03	91.53	5490.79	1.60	10.89	18401.83	1.58	100.24
	800	227.43	2.16	45.09	1029.62	1.35	801.49	1289.15	2.09	49.89	6699.83	1.46	875.41
	1600	76.02	1.58	194.65	267.19	1.95	6468.44	416.88	1.63	214.64	1650.75	2.02	7044.59
		$T=2400$						$T=2600$					
	100	27600.67	—	0.46	80217.69	—	0.76	2900.47	—	0.50	97113.69	—	0.83
	200	11820.57	1.22	2.42	80035.00	0.00	10.51	2046.62	0.50	2.65	97071.21	0.00	11.36
	400	3459.49	1.77	11.94	11016.22	2.86	108.51	806.98	1.34	13.06	5338.06	4.18	118.52
	800	765.42	2.18	54.73	4172.68	1.40	950.33	189.64	2.09	59.89	1459.04	1.87	1043.83
	1600	244.95	1.64	235.22	1060.75	1.98	7651.39	65.09	1.54	257.04	327.07	2.16	8422.95
		$T=2700$						$T=2900$					
	100	506.29	—	0.52	99018.36	—	0.86	578.80	—	0.56	99364.83	—	0.92
	200	296.52	0.77	2.76	98926.90	0.00	11.78	160.35	1.85	2.98	99273.19	0.00	12.63
	400	132.14	1.17	13.62	1177.50	6.39	125.50	77.46	1.05	14.73	86.15	10.17	140.78
	800	32.99	2.00	62.44	287.70	2.03	1107.61	20.00	1.95	67.57	16.84	2.36	1241.75
	1600	11.32	1.54	267.94	62.18	2.21	8938.30	9.20	1.12	290.11	5.94	1.50	10008.14
$m=3$,		$T=400$						$T=600$					
$\nu=3$	100	2360.54	—	0.07	1234.68	—	0.12	12307.41	—	0.11	3938.74	—	0.18
	200	588.13	2.00	0.37	507.41	1.28	1.63	1976.95	2.64	0.57	1351.61	1.54	2.45
	400	192.11	1.61	1.77	126.38	2.01	16.78	475.35	2.06	2.71	503.28	1.43	25.19
	800	58.33	1.72	8.34	53.63	1.24	146.45	138.80	1.78	12.65	171.59	1.55	219.82
	1600	19.63	1.57	35.31	13.49	1.99	1201.02	43.02	1.69	53.03	50.80	1.76	1795.61
		$T=800$						$T=1000$					
	100	9829.85	—	0.14	12258.41	—	0.23	8640.38	—	0.18	8186.72	—	0.28
	200	3098.79	1.67	0.74	3561.14	1.78	3.18	2138.93	2.01	0.94	2719.87	1.59	3.98
	400	800.36	1.95	3.62	1237.34	1.53	32.60	499.20	2.10	4.55	982.36	1.47	40.89
	800	226.01	1.82	16.95	407.87	1.60	284.42	135.84	1.88	21.40	329.44	1.58	357.06
	1600	68.59	1.72	71.10	119.90	1.77	2317.33	40.22	1.76	89.83	97.92	1.75	2904.90
		$T=1000$						$T=1300$					
	100	6613.15	—	0.20	8544.06	—	0.31	834.95	—	0.24	2942.87	—	0.38
	200	1750.78	1.92	1.03	2650.78	1.69	4.39	295.21	1.50	1.23	797.33	1.88	5.42
	400	398.99	2.13	5.02	936.43	1.50	45.20	78.21	1.92	6.03	258.01	1.63	56.12
	800	106.99	1.90	23.63	311.77	1.59	394.82	20.99	1.90	28.32	85.78	1.59	490.56
	1600	31.13	1.78	99.26	92.82	1.75	3210.16	6.13	1.78	118.78	25.74	1.74	3990.47

TABLE 3. Example 3: approximate L^1 errors (e_M, figures to be multiplied by 10^{-6}), convergence rates (θ_M), and CPU times (cpu).

by Spanish MINECO project MTM2017-83942-P and Conicyt (Chile), project PAI-MEC, folio 80150006. LMV is supported by Fondecyt project 1181511. RB and LMV are also supported by BASAL project PFB03 CMM, Universidad de Chile and Centro de Investigación en Ingeniería Matemática (CI^{2}MA), Universidad de Concepción, and by the INRIA Associated Team "Efficient numerical schemes for non-local transport phenomena" (NOLOCO; 2018–2020).

REFERENCES

[1] J.A. Carrillo, A. Chertock, Y. Huang, *A finite-volume method for nonlinear nonlocal equations with a gradient flow structure*, Commun. Comput. Phys. vol. 17 (2015) pp. 233–258.

[2] J.L. Vázquez, The porous medium equation, Oxford University Press, Oxford, 2007.

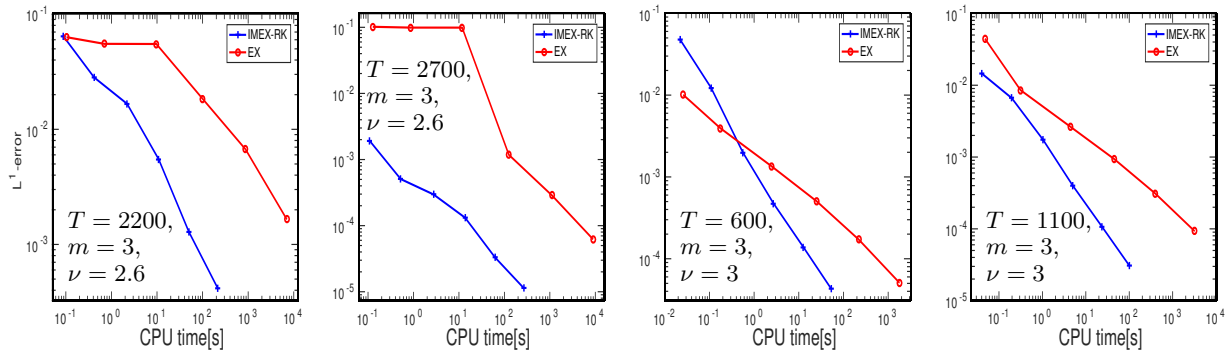

FIGURE 8. Example 3: efficiency plots based on numerical solutions for $\Delta x = 2L/M$ with $L = 15$ and $M = 100$, 200, 400, 800, and 1600.

	IMEX-RK			Explicit			IMEX-RK			Explicit		
M	e_M	θ_M	cpu [s]	e_M	θ_M	cpu [s]	e_M	θ_M	cpu [s]	e_M	θ_M	cpu [s]
	$T = 0.1$						$T = 0.2$					
50	212.98	—	0.01	233.41	—	0.03	216.19	—	0.01	322.13	—	0.06
100	78.58	1.44	0.03	124.21	0.91	0.15	95.25	1.18	0.05	184.56	0.80	0.31
200	49.13	0.68	0.13	69.55	0.84	2.27	55.49	0.78	0.25	98.93	0.90	4.70
400	20.25	1.28	0.63	25.86	1.43	19.87	27.99	0.99	1.25	58.03	0.77	42.03
800	10.71	0.92	3.04	13.84	0.90	180.65	19.77	0.50	6.07	32.69	0.83	380.37
1600	6.81	0.65	13.83	7.56	0.87	1469.53	15.37	0.36	27.78	19.71	0.73	3162.07
	$T = 0.3$						$T = 0.35$					
50	135.82	—	0.02	310.02	—	0.09	116.01	—	0.02	262.17	—	0.10
100	73.90	0.88	0.07	119.81	1.37	0.48	77.97	0.57	0.08	85.25	1.62	0.57
200	39.87	0.89	0.38	62.97	0.93	7.14	44.10	0.82	0.44	107.80	-0.34	8.36
400	28.08	0.51	1.87	46.22	0.45	64.28	28.49	0.63	2.17	28.58	1.92	75.40
800	22.90	0.29	9.04	30.06	0.62	586.95	25.07	0.18	10.45	25.09	0.19	693.39
1600	20.49	0.16	41.54	23.72	0.34	4969.15	23.75	0.08	47.87	24.19	0.05	5914.65

TABLE 4. Example 4: approximate L^1 errors (e_M, figures to be multiplied by 10^{-3}), convergence rates (θ_M), and CPU times (cpu).

[3] E.F. Keller, L.A. Segel, *Initiation of slime mold aggregation viewed as an instability*, J. Theor. Biol. vol. 26 (1970) pp. 399–415.

[4] D. Benedetto, E. Caglioti, M. Pulvirenti, *A kinetic equation for granular media*, RAIRO Modél. Math. Anal. Numér. vol. 31 (1997) pp. 615–641.

[5] R.J. McCann, *A convexity principle for interacting gases*, Adv. Math. vol. 128 (1997) pp. 153–179.

[6] G. Toscani, *One-dimensional kinetic models of granular flows*, ESAIM: Math. Model. Numer. Anal. vol. 34 (2000) pp. 1277–1291.

[7] J.A. Carrillo, G. Toscani, *Asymptotic L^1-decay of solutions of the porous medium equation to self-similarity*, Indiana Univ. Math. J. vol. 49 (2000) pp. 113–142.

[8] F. Otto, *The geometry of dissipative evolution equations: the porous medium equation*, Comm. Partial Diff. Eqns. vol. 26 (2001) pp. 101–174.

[9] C.M. Topaz, A.L. Bertozzi, M.A. Lewis, *A nonlocal continuum model for biological aggregation*, Bull. Math. Biol. vol. 68 (2006) pp. 1601–1623.

[10] F. Betancourt, R. Bürger, K.H. Karlsen, *A strongly degenerate parabolic aggregation equation*, Commun. Math. Sci. vol. 9 (2011) pp. 711–742.

[11] F. Betancourt, R. Bürger, K.H. Karlsen, *Well-posedness and travelling wave analysis for a strongly degenerate parabolic aggregation equation*. In: T. Li, S. Jiang (eds.), Hyperbolic Problems: Theory, Numerics and Applications. Series in Contemporary Applied Mathematics CAM 17/18, vol. 1. Higher Education Press, Beijing, China (2012) pp. 312–319.

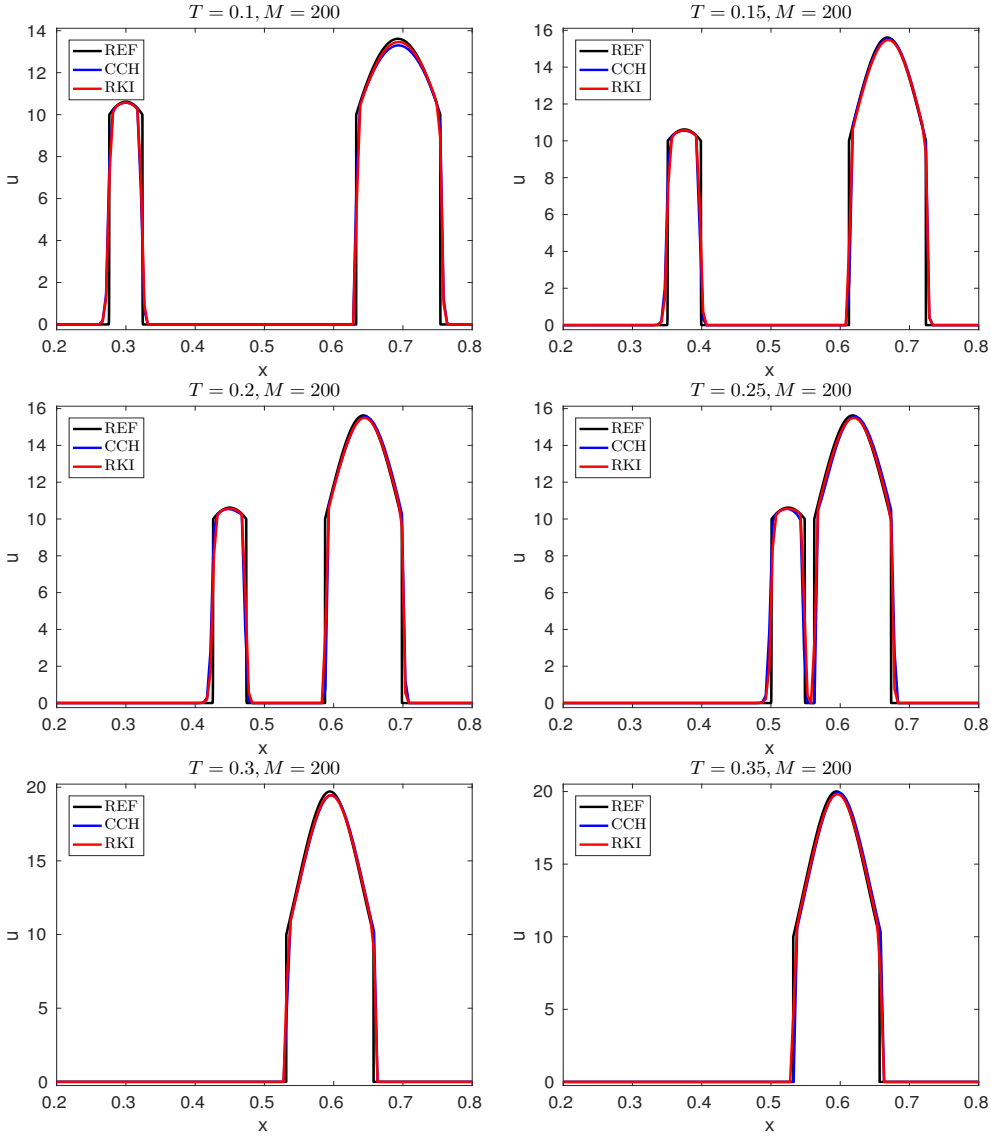

FIGURE 9. Example 4: numerical solution for $\Delta x = L/M$ and $M = 200$.

[12] W. Alt, *Degenerate diffusion equations with drift functionals modelling aggregation*, Nonlin. Anal. Theor. Meth. Appl. vol. 9 (1985) pp. 811–836.

[13] T. Nagai, *Some nonlinear degenerate diffusion equations with a nonlocally convective term in ecology*, Hiroshima Math. J. vol. 13 (1983) 165–202.

[14] T. Nagai, M. Mimura, *Some nonlinear degenerate diffusion equations related to population dynamics*, J. Math. Soc. Japan vol. 35 (1983) pp. 539–562.

[15] T. Nagai and M. Mimura, *Asymptotic behavior for a nonlinear degenerate diffusion equation in population dynamics*, SIAM J. Appl. Math. vol. 43 (1983) pp. 449–464.

[16] T. Nagai and M. Mimura, *Asymptotic behavior of the interfaces to a nonlinear degenerate diffusion equation in population dynamics*, Japan J. Appl. Math. vol. 3 (1986) pp. 129–161.

[17] M. Burger, J.A. Carrillo, M.-T. Wolfram, *A mixed finite element method for nonlinear diffusion equations*, Kinet. Relat. Models vol. 3 (2010) pp. 59–83.

[18] M. Crouzeix, *Une méthode multipas implicite-explicite pour l'approximation des équations d'évolution paraboliques*, Numer. Math. vol. 35 (1980) pp. 257–276.

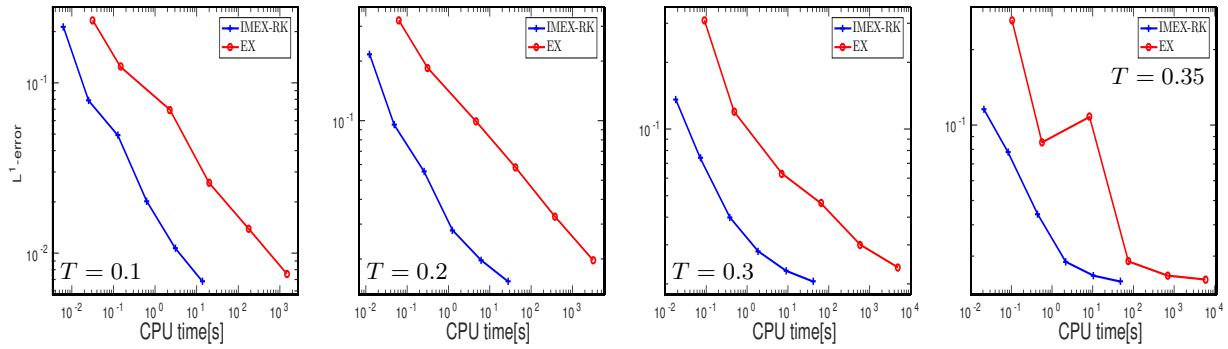

FIGURE 10. Example 4: efficiency plot based on numerical solutions for $\Delta x = L/M$ with $M = 100$, 200, 400, 800, and 1600.

[19] U. Ascher, S. Ruuth, J. Spiteri, *Implicit-explicit Runge-Kutta methods for time dependent partial differential equations*, Appl. Numer. Math. vol. 25 (1997) pp. 151–167.

[20] R. Donat, I. Higueras, *On stability issues for IMEX schemes applied to 1D scalar hyperbolic equations with stiff reaction terms*, Math. Comp. vol. 80 (2011) pp. 2097–2126.

[21] L. Pareschi, G. Russo, *Implicit-Explicit Runge-Kutta schemes and applications to hyperbolic systems with relaxation*, J. Sci. Comput. vol. 25 (2005) pp. 129–155.

[22] S. Boscarino, G. Russo, *On a class of uniformly accurate IMEX Runge-Kutta schemes and applications to hyperbolic systems with relaxation*, SIAM J. Sci. Comput. vol 31 (2009) pp. 1926–1945.

[23] S. Boscarino, G. Russo, *Flux-explicit IMEX Runge-Kutta schemes for hyperbolic to parabolic relaxation problems*, SIAM J. Numer. Anal. vol. 51 (2013) pp. 163–190.

[24] S. Boscarino, P.G. LeFloch, G. Russo, *High order asymptotic-preserving methods for fully nonlinear relaxation problems*, SIAM J. Sci. Comput. vol. 36 (2014) pp. A377–A395.

[25] S. Boscarino, F. Filbet, G. Russo, *High order semi-implicit schemes for time dependent partial differential equations*, J. Sci. Comput. vol. 68 (2016) pp. 975–1001.

[26] C.A. Kennedy, M.H. Carpenter, *Additive Runge-Kutta schemes for convection-diffusion-reaction equations*, Appl. Numer. Math. vol. 44 (2003) pp. 139–181.

[27] X. Zhong, *Additive semi-implicit Runge-Kutta methods for computing high-speed nonequilibrium reactive flows*, J. Comput. Phys. vol. 128 (1996) pp. 19–31.

[28] R. Bürger, P. Mulet, L.M. Villada, *Regularized nonlinear solvers for IMEX methods applied to diffusively corrected multi-species kinematic flow models*, SIAM J. Sci. Comput. vol. 35 (2013) pp. B751–B777.

[29] R. Bürger, P. Mulet, L. Rubio, M. Sepúlveda, *Linearly implicit-explicit schemes for the equilibrium dispersive model of chromatography*, Appl. Math. Comput. vol. 317 (2018) pp. 172–186.

[30] R. Donat, F. Guerrero, P. Mulet, *Implicit-explicit methods for models for vertical equilibrium multiphase flow*, Comput. Math. Appl. vol. 68 (2014) pp. 363–383.

[31] B. van Leer, *Towards the ultimate conservative finite difference scheme, V. A second order sequel to Godunov's method*, J. Comput. Phys. vol. 32 (1979) pp. 101–136.

[32] J. von zur Gathen, J. Gerhard, Modern Computer Algebra, Cambridge University Press, Cambridge, second edition, 2003.

[33] S. Gottlieb, C.-W. Shu, E. Tadmor, *Strong stability-preserving high-order time discretization methods*, SIAM Rev. vol. 43 (2001) pp. 89–112.

[34] J.M. Ortega, W.C. Rheinboldt, Iterative solution of nonlinear equations in several variables, Academic Press, New York-London, 1970.

[35] B. Engquist, S. Osher, *One-sided difference approximations for nonlinear conservation laws*, Math. Comp. vol. 36 (1981) pp. 321–351.

[36] M.G. Crandall, A. Majda, *Monotone difference approximations for scalar conservation laws*, Math. Comp. vol. 34 (1980) pp. 1–21.

Centro de Investigación en Ingeniería Matemática (CI^{2}MA)

PRE-PUBLICACIONES 2018

2018-09 Jay Gopalakrishnan, Manuel Solano, Felipe Vargas: *Dispersion analysis of HDG methods*

2018-10 Franco Fagnola, Carlos M. Mora: *Bifurcation analysis of a mean field laser equation*

2018-11 David Mora, Iván Velásquez: *A virtual element method for the transmission eigenvalue problem*

2018-12 Alfredo Bermúdez, Bibiana López-Rodríguez, Rodolfo Rodríguez, Pilar Salgado: *Numerical solution of a transient three-dimensional eddy current model with moving conductors*

2018-13 Raimund Bürger, Enrique D. Fernández Nieto, Victor Osores: *A dynamic multilayer shallow water model for polydisperse sedimentation*

2018-14 Antonio Baeza, Raimund Bürger, Pep Mulet, David Zorío: *Weno reconstructions of unconditionally optimal high order*

2018-15 Veronica Anaya, Mostafa Bendahmane, David Mora, Mauricio Sepúlveda: *A virtual element method for a nonlocal FitzHugh-Nagumo model of cardiac electrophysiology*

2018-16 Tomás Barrios, Rommel Bustinza: *An a priori error analysis for discontinuous Lagrangian finite elements applied to nonconforming dual mixed formulations: Poisson and Stokes problems*

2018-17 Raimund Bürger, Gerardo Chowell, Elvis Gavilán, Pep Mulet, Luis M. Villada: *Numerical solution of a spatio-temporal predator-prey model with infected prey*

2018-18 Javier A. Almonacid, Gabriel N. Gatica, Ricardo Oyarzúa, Ricardo Ruiz-Baier: *A new mixed finite element method for the n-dimensional Boussinesq problem with temperature-dependent viscosity*

2018-19 Antonio Baeza, Raimund Bürger, María Carmen Martí, Pep Mulet, David Zorío: *Approximate implicit Taylor methods for ODEs*

2018-20 Raimund Bürger, Daniel Inzunza, Pep Mulet, Luis M. Villada: *Implicit-explicit schemes for nonlinear nonlocal equations with a gradient flow structure in one space dimension*

Para obtener copias de las Pre-Publicaciones, escribir o llamar a: Director, Centro de Investigación en Ingeniería Matemática, Universidad de Concepción, Casilla 160-C, Concepción, Chile, Tel.: 41-2661324, o bien, visitar la página web del centro: `http://www.ci2ma.udec.cl`







Centro de Investigación en
Ingeniería Matemática (CI²MA)
Universidad de Concepción

Casilla 160-C, Concepción, Chile
Tel.: 56-41-2661324/2661554/2661316
http://www.ci2ma.udec.cl